Studies on cortical excitability regulation and systemic interference effects of transcranial direct current stimulation

Thesis submitted in partial fulfillment
of the requirements for the degree of

MS by Research
in
Electronics and Communication Engineering

By

Mehak Sood
201234002
mehak.sood@research.iiit.ac.in

International Institute of Information Technology
Hyderabad - 500 032, INDIA
November 2016

International Institute of Information Technology
Hyderabad, India

CERTIFICATE

It is certified that the work contained in this thesis, titled "*Studies on cortical excitability regulation and systemic interference effects of transcranial direct current stimulation* " by **Mehak Sood**, has been carried out under my supervision and is not submitted elsewhere for a degree.

Date	Adviser: Dr. Shubhajit Roy Chowdhury
Date	Co-Advisor: Dr. Rahul Shrestha
Date	Co-Advisor: Dr. Anirban Dutta

To my Family

Acknowledgements

I am using this opportunity to express my gratitude to everyone who supported me throughout the course of this research project.

First and foremost, I would like to express my deepest gratitude to my advisor **Dr. Shubhajit Roy Chowdhury** for providing me the opportunity to pursue this research and for constantly guiding and supervising me with his immense knowledge in the field of Biomedical Engineering. Also I would like to acknowledge the intellectually fertile environment that IIIT- H has given me for pursuing my studies. The experiences that I gathered during my stay here will stay with me forever.

I sincerely thank **Dr. Anirban Dutta**, INRIA starting research scientist, DEMAR team for constantly helping me with my countless queries throughout this project. I also wish to acknowledge **Dr. Abhijit Das**, Institute of Neurosciences- Kolkata for successful completion of this project with his clinical expertise. I would also like to thank **Dr. Rahul Shrestha** for his support and guidance whenever it was needed.

My thanks and appreciations also go to **Mr. Utkarsh Jindal,** who willingly helped me out with his abilities throughout the project.

I attribute the completion of this research study to the blessings, moral support, love and affection of my parents, my sister and my brother as well. They have always been a major source of strength and motivation.

Lastly I express my profound thanks to all those who have helped me in the realization of this work.

Abstract

The past decade has witnessed a significant improvement in neuroimaging technologies and analysis methods in order to observe and measure brain activity. The advances in the understanding of how the brain is organized is the key to progress in fighting neurological disorders. The efforts to find ways to detect and diagnose these impairments depend largely on the data that we are able to obtain about cerebral hemodynamics, fluctuations, structural changes and the associated cortical activities in the brain.

The aim of this thesis is to develop innovative methodologies for examining cortical excitability regulation particularly for stroke patients during transcranial direct current stimulation (tDCS) with the help of Near Infrared Spectroscopy (NIRS) and Electroencephalography (EEG) combined brain imaging. EEG is an electrophysiological method that measures the electrical neural activity directly while NIRS is a method that measures the brain activity indirectly through hemodynamic responses associated with neuron behavior. Transcranial direct current stimulation (tDCS) is a non-invasive technique of modulating brain activity that delivers low intensity direct current to cerebral cortex. It is widely used for stimulating or inhibiting spontaneous neuronal activity.

The alterations in cerebrovascular hemodynamics caused by tDCS can be studied through functional NIRS. A low cost tDCS device was developed and integrated with the custom built NIRS data acquisition device to study the effects of electrical stimulation on brain in patients for prediction of neurological disorders such as ischemic stroke. The NIRS – tDCS device was taken for clinical validation at Institute of Neurosciences, Kolkata and it proved to be a good predictor of cerebral vascular status. It can be used for possible identification of acute stroke. The tDCS – NIRS protocol was then further extended to tDCS-NIRS-EEG protocol.

It was further investigated that the application of tDCS on cerebral site causes systemic interference in the superficial layers of the head. Due to this, there were some fluctuations found in NIRS measurements. The anterior temporal artery tap technique is discussed in the thesis to remove these fluctuations, which may also be able to classify carotid stenosis, external carotid artery stenosis, and internal carotid artery stenosis patients using the laterality in the hemodynamic response evoked by anodal tDCS both at the brain as well as at the superficial layers. These findings may have important implications for both prognosis and rehabilitation of patients with intracranial stenosis.

The EEG and NIRS have different spatial and temporal resolutions, the online tracking of the relation between EEG and NIRS data acquired simultaneously during tDCS has not been investigated earlier. This could provide a sensitive means to monitor the tDCS neuro-modulatory effect. A Kalman filter based approach for online parameter estimation of an autoregressive model to track the relation between tDCS induced cortical neural activity leading to changes in EEG power spectrum and oxy Hemoglobin signals.

This new online NIRS EEG tracking method may allow quantitative assessment of the existence of a coupling relationship between electrophysiological and hemodynamic response to tDCS, which could be used to monitor tDCS neuro-modulatory effect in health and disease.

Contents

Chapter Page

List of Figures

Figure Page

List of Tables

Table Page

Chapter 1

Introduction

Stroke is defined as an acute neurological dysfunctionality originated from impairments in the vascular system. It is associated with a sudden development of clinical signs of brain function disorders, lasting more than a day. Ischemic stroke is a type of stroke that occurs due to lack of blood flow to a part of brain. It is the leading cause of morbidity and long term disability across the world, and is among the leading causes of death. Stroke accounts for nearly 10% of deaths and about 5 % of health care costs. Due to high prevalence of stroke and enormous cost of its management, even the strategies with modest benefits are worth pursuing.

Transcranial direct current stimulation (tDCS) is an emerging technique of noninvasive brain stimulation that has been found useful in examining the cortical function in normal subjects and in facilitating treatments of various neurological disorders. Another therapeutic modality called, Transcranial Magnetic Stimulation (TMS) is also useful in monitoring patients after a stroke but it is not a portable/mobile technology and is expensive. In contrast, tDCS has some advantages, being portable, more economical and easy to operate. It causes polarity dependent effects, leading to increase/decrease in cortical excitability. The idea is that electric therapy may make the brain more plastic and better able to compensate for damaged connections.

1.1 Background

The idea of electrical therapy has existed over 100 years. There were a couple of experiments that were performed before the 19th century using the technique of Transcranial Direct Current Stimulation (tDCS) that tested animal and human electricity. Two researchers Lugi Galvani and Alessandro Volta used tDCS in their explorations of the source of animal-cell electricity. In 1801, Galvani's nephew Giovanni Aldini successfully used current stimulation to improve the mood of melancholy patients. In 1960's, a great researcher DJ Albert proved that the current stimulation could affect the functionality of brain by changing the cortical excitability.

Recently, there has been a rise in interest in tDCS technology as it offers wide applications in the area of Neuro-recovery. It is been encouraged by an increased interest in understanding of basic brain functionality, related therapies as well as new brain imaging techniques such as fMRI, fNIRS and TMS.

Also, attaining upper limb functional recovery has become an ambitious goal for the health care professionals for overcoming various neurological disorders. Manual facilitation, electrical muscle stimulation and functional rehabilitation exercises are all core components of neurorehabilitation and tDCS offers wide application in neurorehabilitation for stroke patients. It has the ability to improve hand function of stroke patients by induction of relatively weak constant current flow to the motor cortex via the scalp.

1.2 Literature Review

Although research has been going on in demonstrating tDCS effects on cognitive functionality, it is still not an FDA-approved technique. There are tDCS administration devices in which some of them are FDA cleared for cortical stimulation (e.g. http://www.fisherwallace.com/) but many non FDA cleared versions also. All of them vary in waveform, frequency, constant current vs. constant voltage, as well as other parameters. It is important to know that the devices have different specifications and are used for different applications [1]. tDCS is still an experimental form of brain stimulation, which potentially has several advantages over other brain stimulation techniques. There are other non-invasive brain stimulation techniques such as transcranial electrical stimulation (TES) and transcranial Magnetic stimulation (TMS) [2] but tDCS differs from these techniques.

TMS is done by passing a strong and brief electric current through an insulated wire coil placed on the skull. This current produces a transient magnetic field, which propagates in space and induces a secondary current in the brain that causes depolarizing of neurons when the coil is placed over subject's head. Depending on the frequency, strength of the magnetic field and the duration of stimulation, TMS can activate or suppress activity in cortical regions. tDCS is performed by passing low intensity DC current by placing two electrodes on the scalp. An active electrode is placed on the site overlying the cortical target, and a reference electrode is usually placed over the contralateral supraorbital area. tDCS can be used to manipulate brain excitability via membrane polarization: cathodal stimulation hyperpolarizes, while anodal stimulation depolarizes the resting membrane potential, whereby the induced after-effects depend on polarity, duration and intensity of the stimulation. Differences between tDCS and TMS include presumed mechanisms of action, with TMS acting as neuro-stimulator and tDCS as neuro-modulator [2]. Moreover, TMS protocols are better established, TMS has better spatial and temporal resolution [2][3], but tDCS has the advantage to be easier to use in double-blind or sham-controlled studies and easier to apply concurrently with behavioral tasks. It does not induce neuronal firing by supra-threshold neuronal membrane depolarization but rather modulates spontaneous neuronal network activity [3][4]. It is cheap, non-invasive, painless and safe. It is

also easy to administer and the equipment is easily portable. Furthermore, Due to the large size of the magnetic coils in TMS, targeting very specific areas of the brain is quite difficult. There is a need to remain completely still during TMS whereas with tDCS the electrodes used to incite stimulation are secured directly against the scalp using a headband or positioning strap, which allows the individual to move about if they desire to do so. When targeting specific areas, tDCS is often used because of its ability to accommodate small electrodes, which can be placed directly on top of the desired stimulation area. TMS induces intense itching and pain sensations over the stimulation site whereas tDCS causes slight itching or tingling on the scalp when it is applied which gradually fades away [3].

The long term effects of tDCS, both positive and negative are still under speculation [1][5]. In the past 15 years, the physiological mechanism of action due to tDCS have been intensively investigated for giving it support in its various applications in clinical neuropsychiatry and rehabilitation [6][7][8]. There has been an exponential rise in the number of studies employing transcranial direct current stimulation (tDCS) as a means of gaining a systems-level understanding of the cortical substrates underlying behavior. Several studies showed that tDCS could induce specific changes in neuropsychological, psychophysiological and motor activity as a function of targeted brain areas [9][10][11]. tDCS is being increasingly explored for the treatment for neurological and psychiatric symptoms and has shown efficacy on symptoms of depression, bipolar disorder, schizophrenia, Alzheimer's disease, Parkinson's disease, epilepsy, stroke and auditory hallucinations [12][13].

The conventional way to perform tDCS is by putting a positive electrode over some part of brain that is to be stimulated and a negative electrode over the part that is to be inhibited. However, the amount of current flowing to a given part of the brain depends critically on the geometry of the whole set up. The variations in the bumps on the scalp and the exact position of electrodes makes a noticeable difference in how much current goes where. The City University of New York invented the High-Definition transcranial Direct Current Stimulation (HD-tDCS). The 4x1 HD-tDCS montage categorically transformed the possibilities with non-invasive neuromodulation and allows for precise targeting of specific cortical structures [9] [14]. Therefore, in applications where more precision is required, the stimulation can be tailored using HD-tDCS (High Definition tDCS) (Fig 1.1) which consists of four or more electrodes and computer models of current flow. Also, In a pilot study, HD-tDCS was found to have a more effective and long lasting motor cortex excitability [5] [15]. However, clinical

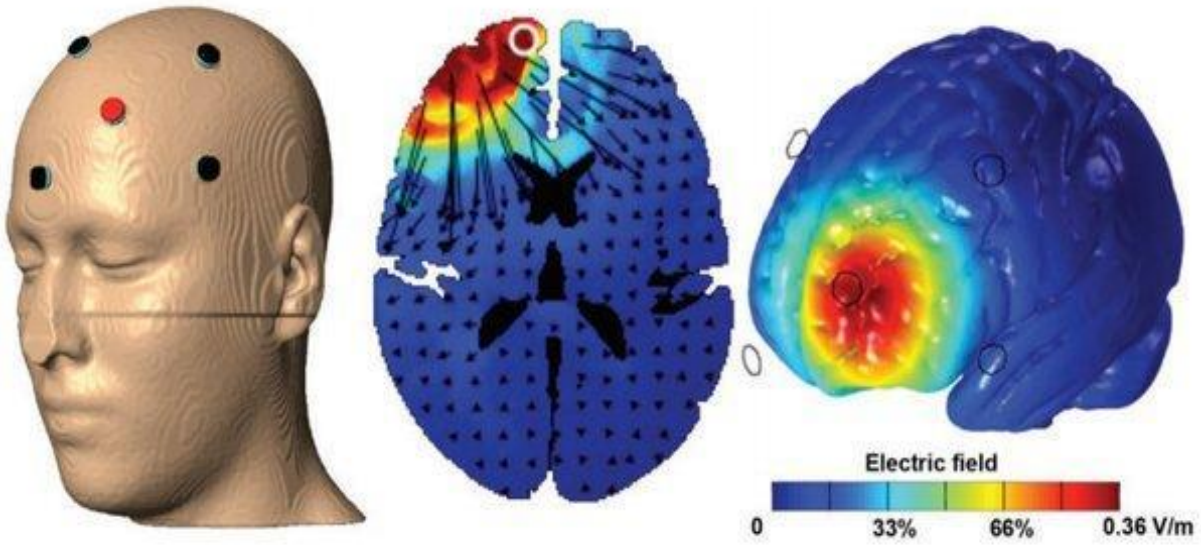

Fig 1.1 HD-tDCS to maximize current at the target

benefits of HD-tDCS in psychiatric conditions has not yet been reported. Also, novel approaches with regard to types of electric currents have been studied, suggesting unique effects on neurons. Transcranial alternating current stimulation (tACS) uses fluctuating and alternating polarity of current with a certain frequency, instead of direct current, and is suggested to produce brain oscillations [16]. Transcranial random noise stimulation (tRNS) is a special form of tACS, with a frequency spectrum characteristic of white noise [17].The reader is suggested to consult for more reviews on the action and development of new tDCS technologies [4] [18].

The maximum current intensity that is generally used in tDCS is 2 mA. However, a higher current density of 25mA/cm^2 has been applied on animals and it did not induce lesions in the brain tissue, meaning that limits well above those applied in humans would not result in adverse effects, thereby proving it to be a safe technique [10] [19] [20].

1.3 Motivation

The rediscovery of tDCS in recent years [11] has led to an escalation of research on brain and cognitive development, both in healthy adults and in patients with neurological impairments. Although, the early motivating rationale behind use of tDCS was its effectiveness in the therapeutic treatment of neuropsychiatric diseases, but nowadays tDCS is used in improvement of cognitive functioning in healthy adults (e.g., fatigue, stress) as well as those undergoing brain disorders (e.g. Stroke, Transient Ischemic Attack, Loss of Motor functionality). The major effect

of tDCS is to modulate cortical excitability, but the way in which such modulation translate into improvement in performance is still not well understood. Also, the after-effects of tDCS is an interesting aspect that is related to neuromodulation [6]. The duration of this after-effects depends on the length of stimulation as well as the intensity of stimulation [6]. One of the unsolved issue is the role of hemodynamics in tDCS after-effects [21]. To understand the underlying mechanism of neuromodulation is currently the object of much research interest. Thus, combining tDCS with the emerging multimodal neuroimaging techniques such as NIRS, EEG and fMRI can enhance the knowledge of tDCS neuro-modulatory effects on the brain and can help in diagnosis and treatments of various neurological disorders. In this thesis, we have investigated the neuro-modulatory effects of tDCS using NIRS and EEG joint imaging and the main focus is on patients suffering from acute stroke.

The neuro-modulatory effects of tDCS are reflected in NIRS and EEG readings. NIRS measures the neural activity indirectly through Hemodynamic Reponses associated with neuron behavior, whereas EEG measures the electrical neural activity directly. Both of these modalities possess different spatial and temporal features. The combination of these two modalities therefore offers the possibility to examine the brain's functionality more comprehensively. Also, combining NIRS and EEG is certainly advantageous because of the comparatively low cost and portability in contrast to other imaging techniques such as MRI (Magnetic Resonance), MEG or Positron Emission Tomography.

1.4 Scope of Present Work

In this thesis, we have developed a computational model for understanding the relationship between simultaneously acquired electroencephalographic (EEG band-power <12Hz) and near infrared spectroscopic (O2Hb) data during anodal tDCS. The online parameter estimation using this model was performed with a Kalman filter and this technique was found to be sensitive for quantitative and qualitative assessment of the neuro-modulatory effects of non-invasive brain stimulation (NIBS) in health and disease. The brain imaging techniques – NIRS and EEG have been used for examining the neural activity due to tDCS. NIRS is a fairly inexpensive, low power optical imaging tool in contrast to fMRI brain imaging technique. It has become a relevant research tool in neuroscience for its effectiveness in measuring the hemodynamic responses from neural activity. EEG also is a non-invasive brain machine interface, and is popular mainly due to its fine temporal resolutions, ease of use, portability and low set-up cost [22]. For clinical use in neurology the work in this thesis can translate into the option of providing a bed-side point of care setup for the brain, broadly available at comparatively low costs.

1.5 Organization of Thesis

Chapter 2 describes the implementation of tDCS, placement of tDCS electrodes and its integration with the NIRS Data acquisition device to study the effects of tDCS on cortical excitability. The validation of tDCS –NIRS protocol is also presented.

Chapter 3 discusses a temporal artery tap technique to identify the interference occurring in the superficial layers of head due to application of tDCS using NIRS EEG joint imaging.

Chapter 4 discusses the development of an Autoregressive (ARX) model for online tracking of the relation between electrophysiological (EEG) and hemodynamic (fNIRS) data acquired simultaneously from the human cortex during tDCS, which could be used to sensitively monitor the tDCS neuro-modulatory effect in health and disease. A computational ARX model is developed in this chapter for online parameter estimation with a Kalman Filter.

Chapter 5 presents the implementation of the approach discussed in Chapter 4. It describes the experiments performed on healthy subjects, the MATLAB simulations and results obtained with this approach.

Chapter- 2

Introduction to Transcranial Direct Current Stimulation (tDCS)

Transcranial Direct Current Stimulation (tDCS) - a technique of noninvasive brain stimulation was first established in neuroscience research in the 1950's and 60's, but has seen a rapid growth particularly in the last 5 years. It has been investigated to be used as a treatment for a variety of conditions such as stroke recovery, depression and pain. In this chapter, we introduce both the theoretical aspects and practical application of tDCS. The integration of tDCS with NIRS and EEG has also been discussed in this chapter.

2.1 tDCS - Theory

tDCS makes use of low intensity electric DC current through the electrodes, creating a flow of electric current in the brain which usually causes a slight itching or tingling sensation on the scalp. Due to very weak currents and the noninvasiveness of tDCS, this technique is suitable for modulation of the cerebral cortex, the most outer part of the brain, which lies closest to the surface electrodes attached to the patients head. The weak DC current applied is strong enough to elicit significant effects on cortical activity. These effects cause the oxygen levels to increase at the stimulated area in the healthy subjects.

tDCS involves use of at least 2 surface electrodes(one anode and one cathode) to deliver a stimulating current to the patient. There are three types of stimulation as discussed below:

Types of Stimulation:

1. Anodal tDCS
2. Cathodal tDCS
3. Sham tDCS

The anodal stimulation is positive (+ve) stimulation that increases the neuronal excitability of the area being stimulated. It has been shown that anodal tDCS enhances activity and excitability of the excitatory pyramidal neuron at a population level in a non-specific manner, where μ rhythm desynchronization as found to be generated [23].

Cathodal Stimulation, also called negative (-ve) stimulation decrease the neuronal excitability of the area being stimulated. It can treat the psychologic disorders that are caused by hyper-activity of an area of the brain. Studies suggest that cathodal tDCS decreases the firing rate of neurons thereby downregulating the activity and excitability of the excitatory pyramidal neuron [24]. Cathodal tDCS induces a decrease in regional cerebral blood flow (rCBF) in cortical & subcortical areas.

Sham stimulation is used as a control in experiments. It emits a brief current and then remains off for the remainder time of stimulation. With sham stimulation, the person receiving the tDCS is unaware of the fact that they are not receiving prolonged stimulation.

By comparing the results in subjects exposed to sham stimulation with the results of subjects exposed to anodal or cathodal stimulation, we can examine the effect caused by anodal/cathodal stimulation.

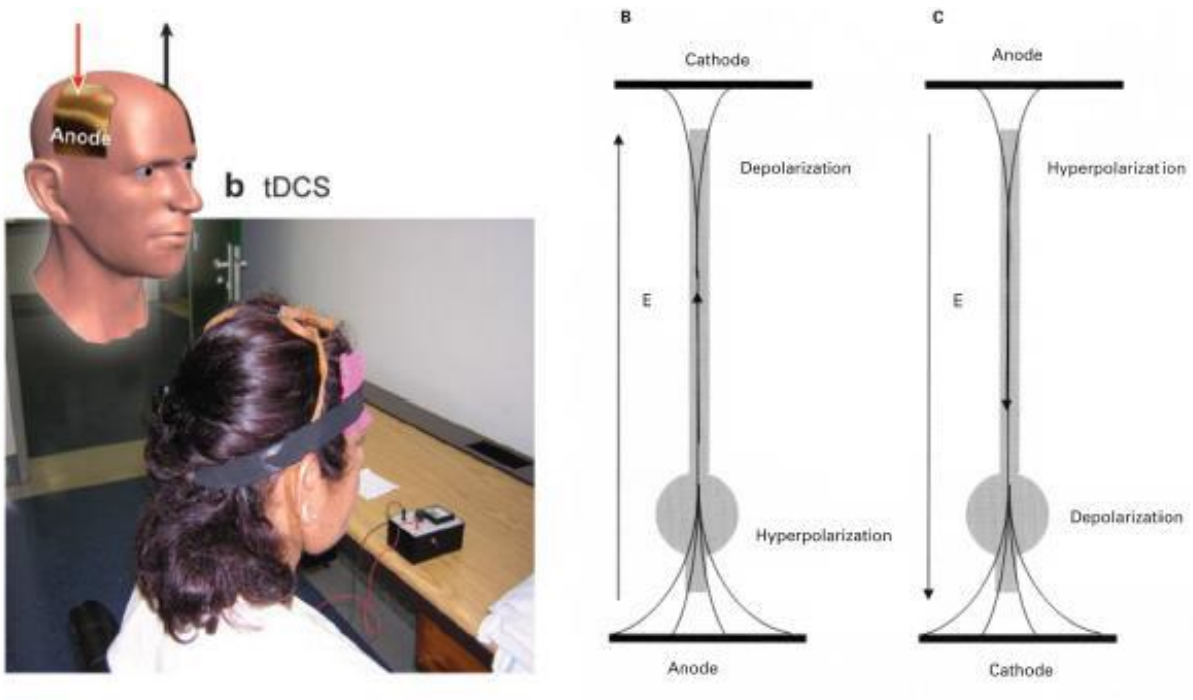

Fig 2.1 Transcranial direct current stimulation (tDCS) is a form of NIBS which uses low DC current delivered directly to the brain area of interest and the modulation of cortical excitability depends on the direction of current flow with respect to the neuronal orientation [25]

2.2 tDCS – Effect on Brain

tDCS – an electrically based intervention directed at the central nervous system level has been investigated to modulate cortical neural activity and is a promising tool to facilitate neuroplasticity.

The Brain is the most complex organ in the human body, comprising of an intricate network of billions of nerve cells, called neurons. These neurons control and react to everything that happens in our bodies. The neurons in your brain communicate to each other using tiny electrical, and chemical impulses called synapses. Electrical synapses, unlike chemical synapses, conduct nerve impulses faster (approximately 10 times faster) and causes vital information to pass from one neuron to another very quickly.

When a stroke strikes, the supply of blood to the part of the brain affected is interrupted, starving it of oxygen causing the surrounding neurons to be seriously damaged or die. It's for this reason stroke victims may lose sensory, cognitive, or motor function. The cells that once carried oxygen to the brain can no longer perform their base function, impairing the local functionality of the brain.

Neuroplasticity refers to the ability of the brain to rewire or reorganize itself after such an injury. It plays a critical role in learning and memory as well as mediating functional recovery from brain lesions like stroke and traumatic brain injuries. Extrinsic strategies to aid favorable modulation of neuroplasticity act as important adjunctive tools of neurorehabilitation. tDCS is an example of a non-invasive technique that can successfully induce neuro-plastic changes in the human brain.

By applying a current in a certain direction, tDCS can effectively increase or decrease electrical polarization (Fig 2.1), affecting the chance that neurons in a given region of the brain will fire depending on the orientation of the subject's synapses and whether a positive or negative current is applied. The potential to decrease neuronal activity seems just as important as the potential to increase it by way of medical and psychiatric applications of the technology. Disorders like schizophrenia, for instance, seem to be linked to over-excitability in certain parts of the brain and can be treated by inhibiting the neuronal activity.

One of the aspects of tDCS is that it has the ability to achieve cortical changes even after the stimulation is ended. The duration of this change depends on the time period of stimulation as well as the intensity of electric current. The effects of stimulation increase as the duration of stimulation increases or the strength of the current increases. The way that the stimulation changes brain function is either by causing the neuron's resting membrane potential to depolarize or hyperpolarize (Fig 2.1). When positive stimulation (anodal tDCS) is delivered, the current causes a depolarization of the resting membrane potential, which increases neuronal excitability and allows for more spontaneous cell firing. When negative stimulation (cathodal tDCS) is delivered, the current causes a hyperpolarization of the resting membrane potential. This decreases neuron excitability due to the decreased spontaneous cell firing.

2.3 Choice of location of electrodes in tDCS

Studies suggest that tDCS is a good approach for studying brain–behavior relationships in patients with lesions, since it has the capacity to systematically modify behavior by inducing changes in underlying brain function. The effect of tDCS on brain differs greatly depending on the area of brain which is targeted for stimulation. Therefore, deciding the placement of electrodes for tDCS is crucial, and must be researched thoroughly before attempting any session.

As it is mentioned in previous section, tDCS uses one anode and one cathode electrode that are placed over the scalp in order to modulate a particular area of the brain. The electrode positioning is determined according to the International 10 -20 of EEG electrodes (Fig 2.2). It is an internationally recognized system to describe the location of scalp sites. The system is based on the relationship between the location of an electrode and the underlying area of cerebral

cortex. The sites are marked in the figure (Fig 2.2 (a)) .Each site is represented by a letter (to identify the lobe) and a number or another letter to identify the hemisphere location. The letters F, T, C, P, and O stand for Frontal, Temporal, Central, Parietal and Occipital. The even numbers (2, 4, 6, 8) refer to the right hemisphere and odd numbers (1, 3, 5, 7) refer to the left hemisphere. The z refers to an electrode placed on the midline. Also note that the smaller the number, the closer the position is to the midline.

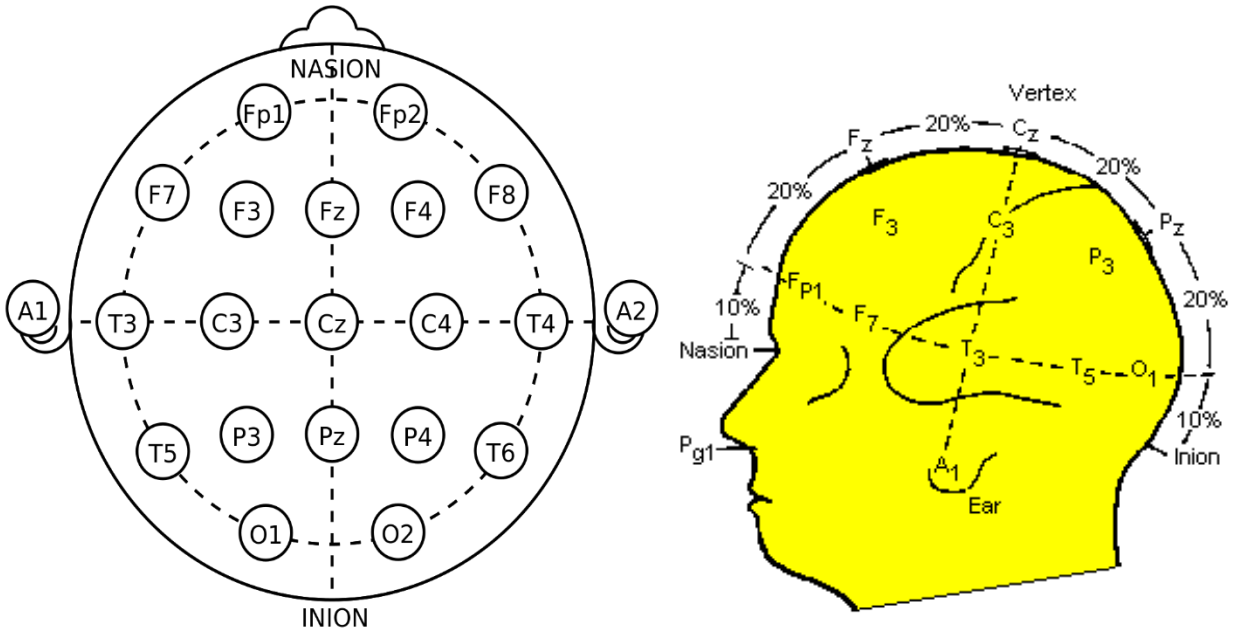

(a) (b)

Fig 2.2 10/20 International system of scalp sites

The DC current is passed between anode (+ve) and cathode (-ve). Under anode, the current flows inward and under cathode, the current flows outward.

The Middle Cerebral Artery (MCA) is the largest cerebral artery that is most commonly affected by a cerebrovascular accident. It is one of the three major paired arteries that supply blood to the cerebrum and is most commonly occluded vessel in ischemic stroke. The tDCS montage was selected based on computational modelling [26] in order to target primarily the outer convex brain territory (superficial divisions) of the MCA. The F3 (left hemisphere) and F4 (right hemisphere) site was chosen as cathode and Cz was chosen as anode for anodal stimulation. Excitation occurs when anode is placed over motor cortex and cathode over supraorbital edge. The anode acts as stimulation spot and cathode as reference electrode.

2.4 Development of NIRS –tDCS DAQ device

2.4.1 Functional Near Infrared Spectroscopy (fNIRS)

Near-infrared spectroscopy (NIRS) is a cerebral monitoring method that noninvasively and continuously measures cerebral hemoglobin oxygenation which is widely used for measurement

of cerebral vascular status under various clinical conditions. Functional near infrared spectroscopy (fNIRS) is based on the optical measurement of changes in tissue oxy-(*HbO*2), and deoxy-(*Hb*) hemoglobin concentration [27] whereas cerebral oximetry is cerebral oxygenation monitoring via near-infrared spectroscopy (NIRS) [28]. The responses measured during fNIRS are usually interpreted in terms of changes in *HbO*2 and *Hb* concentration — a somewhat richer set of variables than those available from basic fMRI. A third hemodynamic variable, *Hb*t, can be derived as the sum of *Hb* and *HbO*2 concentrations, which is considered a good indicator of the variations in the regional cerebral blood volume (CBV) [29].

NIRS instrumentation works on different measuring principles, e.g., continuous wave (CW), frequency domain (FD), and time domain (TD). Absolute concentration measurements may be possible with more expensive TD and FD techniques [30] but quantification was not a crucial factor in our application, since we wanted to detect a relative change in HbO2 and Hb in response to transcranial direct current stimulation rather than to quantify the hemodynamic response in absolute terms.

Continuous wave fNIRS offers a relatively non-invasive, safe, portable and low cost method of monitoring hemodynamic correlate of brain activity and relies on the principle of neurovascular coupling (NVC) [31]. Hemodynamic changes associated with brain activity or more precisely the relationship between local neural activity and cerebral blood flow is termed neurovascular coupling (NVC) [32]. Understanding NVC is important in terms of interpreting the responses acquired during fNIRS especially in the case of measurement in damaged brain such as following a stroke when alterations in the pathophysiological conditions of neurovascular mechanisms may exist [33].

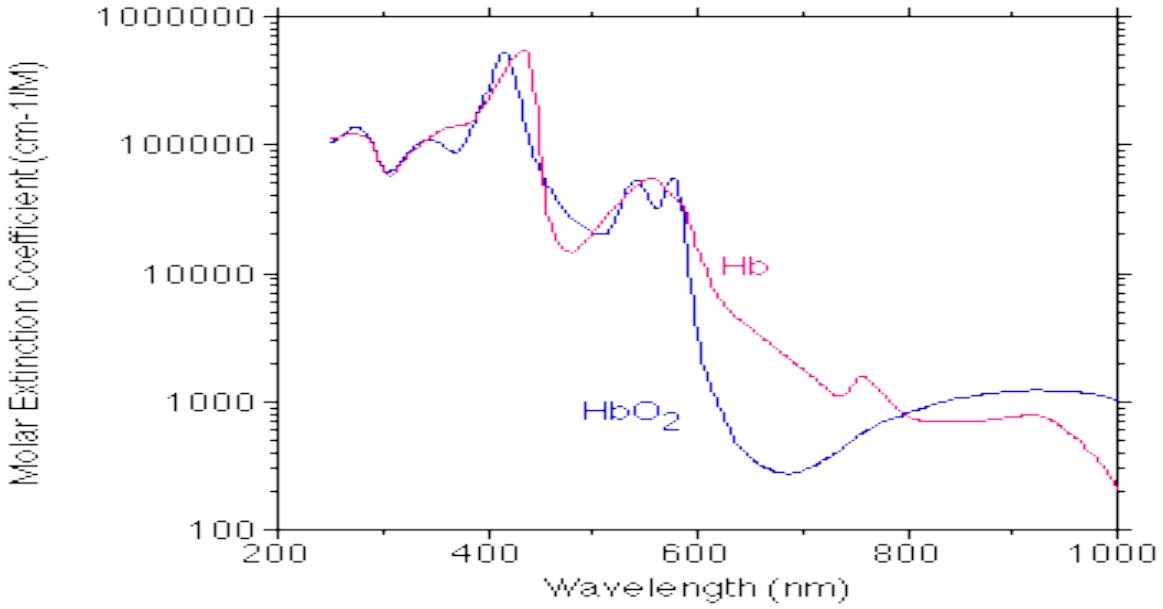

Fig 2.3 Absorption Spectra of Oxy Hb and Deoxy -Hb

NIR light spectrum between 700 to 900 nm is mostly transparent to skin, tissue, and bone, while hemoglobin (Hb) and deoxygenated-hemoglobin (deoxy-Hb) are stronger absorbers of this spectrum.

Differences in the absorption spectra (Fig 2.3) of oxy-Hb and deoxy-Hb enable us to measure relative changes in hemoglobin concentration through the use of light attenuation at multiple wavelengths [34]. Two or more wavelengths are selected, with one wavelength above and one below the isobestic point of 810 nm at which deoxy-Hb and oxy-Hb have identical absorption coefficients (Fig 2.3).

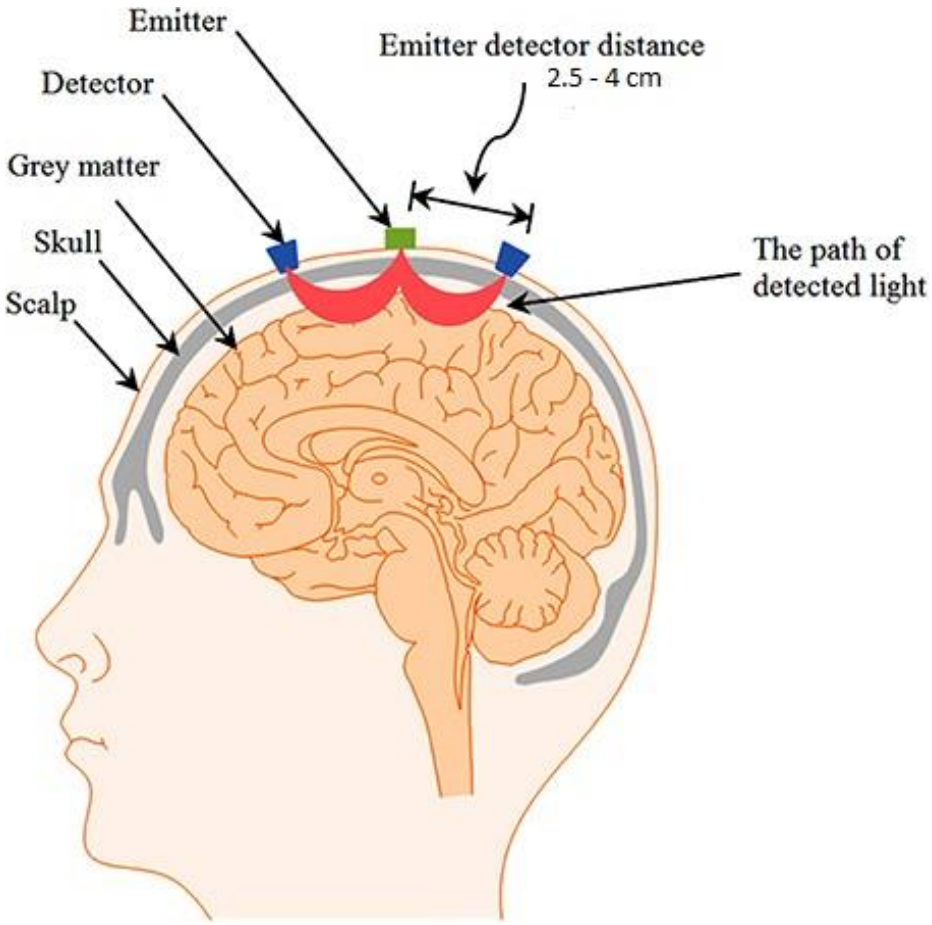

Fig 2.4 Back Scattering by NIRS emitters

Using the modified Beer-Lambert Law (Mbll), relative concentration can be calculated as a function of total photon path length. Typically, the light emitter and detector are placed ipsilaterally on the subjects skull so recorded measurements are due to back-scattered (reflected) light following elliptical pathways (Fig 2.4)

The mBLL relates the chromophore concentration levels to optical absorption values. It can be expressed in terms of the parameters relevant to fNIRS as follows:

$$A_\lambda = \log(\frac{1}{T}) = (a_{\lambda,\,Hb}.[Hb] + a_{\lambda,\,HbO}.[HbO]).B_\lambda.L + G$$

where T is the *transmittance*, which is the ratio of incident power to transmitted power. The term Aλ is termed the *optical density* and it is wavelength specific. The wavelength dependency comes from the wavelength-specific absorption tendencies (represented by the specific extinction coefficients: aλHb, aλHbO) of oxy- and de-oxy-hemoglobin. These values have been experimentally derived and tabulated elsewhere [35]. The term G is used to account for optical losses dues to scattering and is assumed constant over the measurement period. Usually a differencing operation is used to eliminate the effect of scattering to yield:

$$\Delta A_\lambda = a_{\lambda,\,Hb}.\Delta[Hb] + a_{\lambda,\,HbO}.\Delta[HbO]).B_\lambda.L$$

and therefore *changes* in chromophore concentrations are a common measurement made during fNIRS studies.

2.4.2 NIRS DAQ Device

This section describes the development of a 4-channel functional near infrared spectroscopy (fNIRS) based hardware that captures the hemodynamic changes in the frontal cortex of the brain, as a measure of cerebrovascular reserve (CVR), before and after anodal transcranial direct current stimulation. The design of NIRS probes is shown (Fig 2.5). S1, S2 are sources and D1, D2, D3 and D4 are detectors.

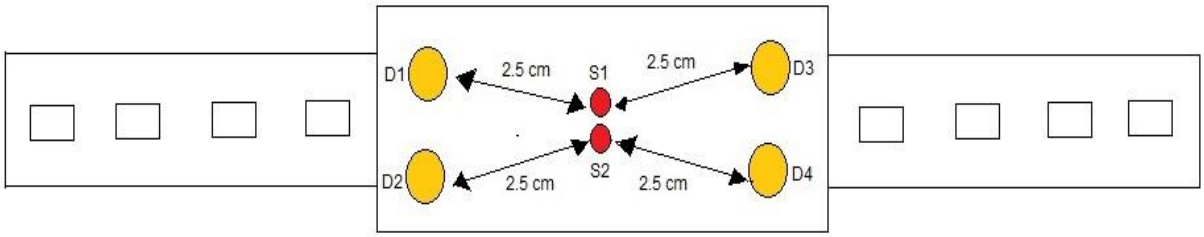

Fig 2.5 NIRS probe

The wavelengths used in the experiment are 770nm and 850nm. The distance between the source and detector is kept at 2.5cm. The signal obtained at 4 channels is high pass filtered (fc = 0.8Hz) and amplified by an instrumentation amplifier followed by a fourth order Butterworth low pass filter (fc = 8.86Hz). The block diagram of the setup is shown (Fig 2.6).

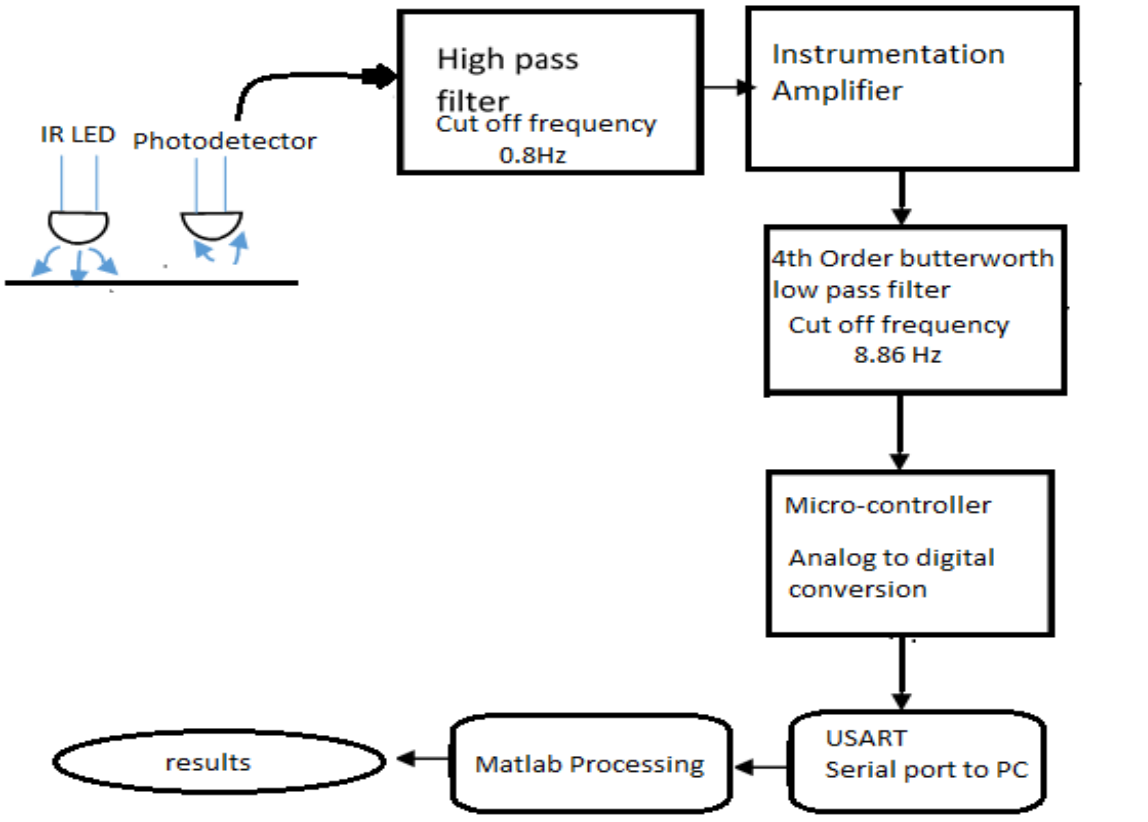

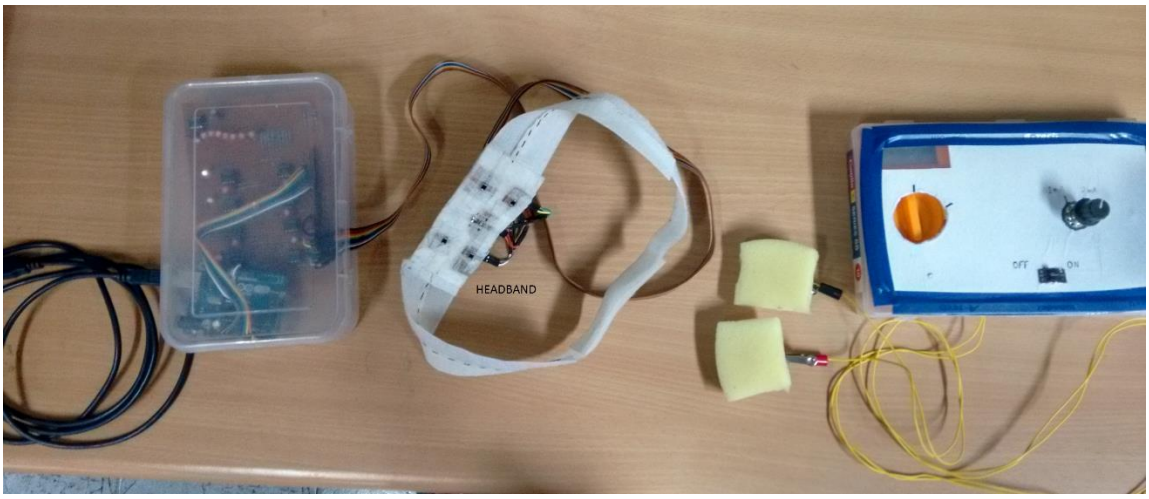

Fig 2.6 NIRS-tDCS setup

.

Differential spectroscopy has been used to obtain relative changes in the concentrations of the two chromophores, viz. oxy-hemoglobin and deoxy-hemoglobin, making it possible to identify whether changes in oxygen saturation result from changes in blood volume or changes in oxygen consumption. Modified Beer Lambert's Law has been used to relate the chromophore

concentration to the optical absorption values. An increase/decrease in blood volume causes an increase/decrease in total hemoglobin concentration which in return causes a change in oxygen saturation. Changes in oxygen consumption are reflected by changes in oxy- and deoxy-hemoglobin concentrations in opposite directions so that the total hemoglobin concentration stays the same. Differential oxyhemoglobin and deoxyhemoglobin concentrations were estimated using modified Beer Lambert's Law

2.4.3 Development of tDCS

The hardware is capable of providing a constant current ranging from 0.25 mA to 2.25 mA. The current is controlled using a three terminal adjustable current source (LM334) and adjusted using a simple analog potentiometer and a digital potentiometer (AD5254 - Analog Devices http://www.analog.com/media/en/technical-documentation/data-sheets/AD5253_5254.pdf).

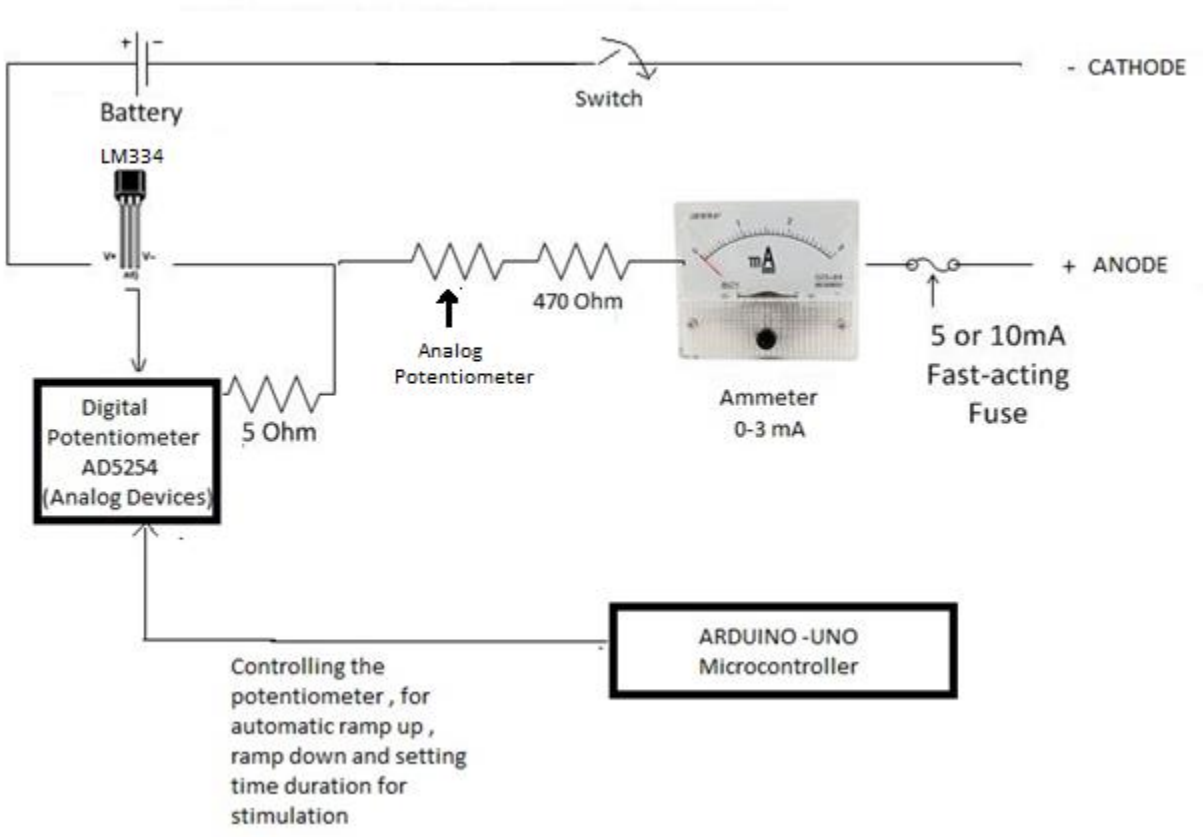

Fig 2.7 tDCS

AD5254 is used for automatic ramp up and ramp down of current and also for storing the duration of stimulation for the patient. The linear ramp up and ramp down of 30 seconds is applied at the beginning and end of stimulation respectively. . The time for which the stimulation lasts can be easily programed from a computer. The device allows adjustment of output current in fine increments (i.e. 0.1 or 0.25 mA steps) for the protection and comfort of the patient. The variation

in resistance of AD5254 for increasing/decreasing the current intensity is programmed using the Arduino – Uno microcontroller. Four values for the duration of stimulation can be stored on the hardware for providing the required stimulation to the patient. The diagram of circuit is shown in Fig. 2.7. In case of abnormal skin sensation due to tDCS, the device is provided with a knob (analog potentiometer) with which the intensity of current can be manually reduced.

Due to ease of availability and economic factors simple sponge electrodes soaked with normal solution (0.9% sodium chloride solution) have been used as anode and cathode [29]. The area of these electrodes is kept to be 5cm×5cm. The saline solution is used to minimize the electrical impedance of the electrode-skin interface and reduce voltage demands for stimulation. Moreover, it removes the possibility of any electrochemical reactions at the electrode-skin interface thereby eliminating the chances of skin lesion.

2. 5 Validation of NIRS – tDCS prototype

Fig 2.8 Experiments conducted at INK, Kolkata

We recruited 14 patients with established and acute ischemic stroke (<1 month) localized to a single hemisphere (10 male and 4 females from age 42 to 73) at the Institute of Neurosciences, Kolkata (Fig 2.8). Subjects were recruited only after ethics approval and experiments were conducted after taking informed consent, conforming to the Declaration of Helsinki. Participants were seated in a quiet room and their eyes were open and fixed on a point on the wall in front of them during the entire experiment. The total testing time was roughly 14 minutes. Anodal tDCS with anode at Cz (international 10-20 system of scalp sites) and cathode over F3 (F4 when monitoring the right side) (Fig 2.9) was conducted with current density maintained at $0.526 A/m^2$.

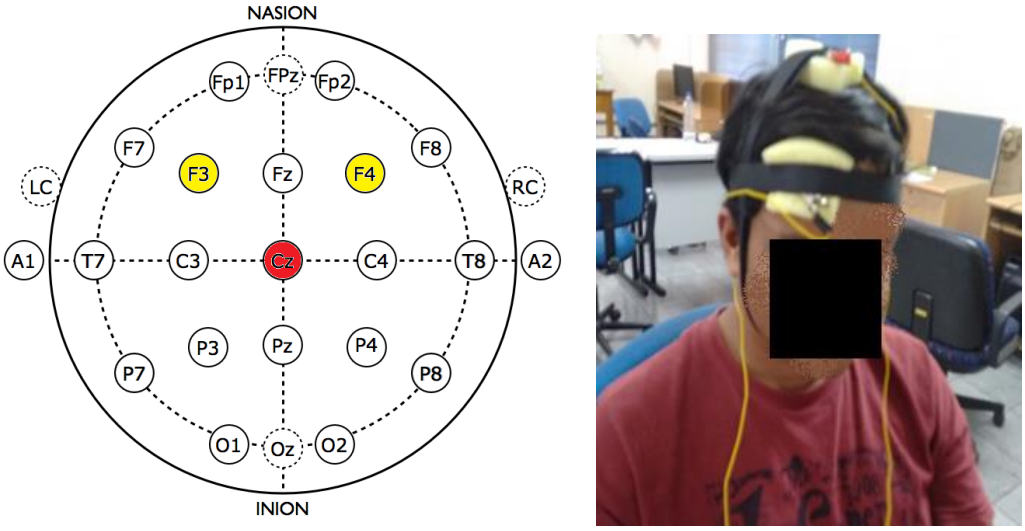

Fig 2.9 tDCS Montage

We observed the results obtained from the experiments performed on these subjects and found that the affected hemisphere of the brain with impaired circulation showed significantly less change in rCBF than the healthy side in response to anodal tDCS. There was significant change in HbO2 in the healthy side (3.43+/- 0.86) but not in side with stroke (0.26 +/- 0.28), $p<0.01$. Fig 2.10 shows the changes that occurred due to the stimulation given by anodal tDCS. To understand the mechanisms underlying NIRS responses elicited with tDCS, a phenomological model was proposed (based on the Friston's model) [7] according to which anodal tDCS cause changes in synaptic transmembrane current resulting in change in CBF via a change in the representative radius of the vasculature, and not in arterial and venous blood pressure difference. Also, it was assumed that the changes from baseline in Hbo2 during anodal tDCS were solely due to local hemodynamic effect induced by anodal tDCS and not due to changes in arterial oxygen concentration.

2.6 Effect of tDCS on NIRS

In the previous section, we proposed a point of care testing device for examining the cerebrovascular status during anodal tDCS. Anodal tDCS has been employed to study the impairments in cerebrovascular reactivity (CVR) through use of NIRS. Thus the combination of NIRS – tDCS could be a good predictor of cerebral vascular status and can be used for stratification and possible identification of acute stroke.

Also, the noninvasiveness and low power make tDCS a rather safe and comfortable experience for both the patient and the operator. Simple electronics keep the cost for tDCS lower than most competitive pharmaceutical therapies and other stimulation technologies like DBS or TMS. In

order to justify this methodology for routine use in clinical population, the effects of tDCS on NIRS measurements also needs to be investigated.

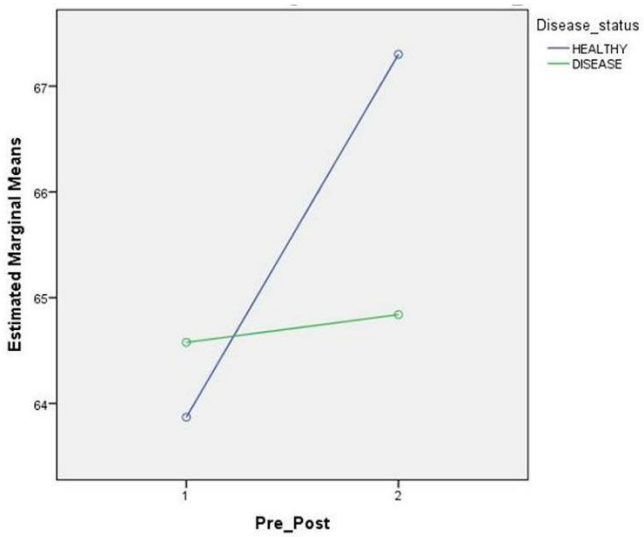

Fig 2.10 Significant change in HbO2 in the healthy side (3.43+/- 0.86) but not in side with stroke (0.26 +/- 0.28), $p<0.01$

The application of tDCS at the site of stimulation causes some artifacts in the NIRS measurements. These artifacts are due to the systemic interference occurring in the superficial layers of the head caused by tDCS. A technique to overcome this issue has been discussed in the chapter 3.

As tDCS is known to modulate cortical neural activity. It can be proved by observing the EEG power spectrum. During neural activity, the electric currents from excitable membranes of brain tissue superimpose at a given location in the extracellular medium and generate a potential which is referred to as EEG (electroencephalogram) when recorded from the scalp. This neural activity is closely related, spatially and temporally to cerebral blood flow (CBF) that supplies glucose via neurovascular coupling. The hemodynamic response to the neural activity is captured by NIRS, which enables continuous monitoring of cerebral oxygenation and blood volume. CBF is increased in brain regions with neural enhanced activity via neurovascular coupling. Thus, the onset effects of tDCS can be captured using NIRS –EEG joint imaging. A computational modelling methodology has been formulated in chapter 4 and chapter 5 for the online tracking of tDCS effects using NIRS-EEG joint imaging.

Chapter 3
Identification of systemic interference due to tDCS using short separation NIRS measurement

The preliminary studies show the feasibility of identifying the lesioned hemisphere in subacute stroke with the low-cost NIRS-tDCS hardware. A significant change in oxy-hemoglobin (HbO2) post-tDCS from pre-tDCS baseline was found for the contra-lesioned (3.43 +- 0.86), but not the lesioned side (0.26 +- 0.28), $p<0.01$. Moreover, the results of the stroke case series showed that anodal tDCS induces a local neurovascular response which may be used for assessing regional NVC functionality.

Transcranial direct current stimulation (tDCS) modulates the cortical neural activity and facilitates neuroplasticity. During neural activity, the electric currents from excitable membranes of brain tissue superimpose at a given location in the extracellular medium and generate a potential, referred as the electroencephalogram (EEG) recorded from the scalp. The respective neural activity is closely related, spatially and temporally, to cerebral blood flow (CBF) that supplies glucose via neurovascular coupling. The hemodynamic response to neural activity can be captured by near-infrared spectroscopy (NIRS), which enables continuous monitoring of cerebral oxygenation and blood volume.

In this chapter, we develop a method for electroencephalography (EEG) - near-infrared spectroscopy (NIRS) based assessment of neurovascular coupling (NVC) during anodal tDCS. In addition, we will address the challenge that remains in removing the systemic interference occurring in the superficial layers of the head that are also affected by tDCS . Here, the importance of integrating short separation NIRS measurements both at the source and at the detector optode has been shown. In this chapter, we present a temporal artery tap technique to identify systemic interference using short separation NIRS measurements. We use NIRS-EEG joint-imaging to measure the changes in mean cerebral hemoglobin oxygen saturation (rSO2) along with the changes in log-transformed mean power of EEG within 0.5Hz-11.25Hz frequency band due to anodal tDCS. We show that the percent change in the mean rSO2 better correlates with the corresponding percent change in log-transformed mean-power of EEG within 0.5Hz-11.25Hz frequency band after removing the systemic contamination using the temporal artery tap method.

3.1 NIRS-EEG/tDCS joint-imaging

We conducted simultaneous recording of NIRS and EEG [18] for evaluation of NVC (see Figure 3.1(a)) on five chronic (>6 months, see Table 3.1) ischemic stroke survivors after obtaining informed consent. The patients had no contraindications to non-invasive brain stimulation. All experiments were conducted in accordance with the Declaration of Helsinki. Here, the NIRS-EEG/tDCS joint-imaging protocol is similar to our prior NIRS-tDCS study [36]

Table 3.1 Subject summary (M: male, F: female, MCA: middle cerebral artery)

Case	Age/Gender	Diagnosis	Year of Stroke
1	68/M	Right MCA Stroke	2010
2	74/F	Left MCA Stroke	2011
3	76/M	Left MCA Stroke	2011
4	72/M	Right MCA Stroke	2012
5	75/M	Right MCA Stroke	2012

Participants were seated in a quiet room and their eyes were open and fixed on a point on the wall in front of them during the entire experiment. PISTIM (Neuroelectrics, Spain) electrodes were placed over F3 (corresponding to the left hemisphere) and F4 (right hemisphere) of the international 10-20 EEG system, and SPONSTIM-25 (Neuroelectrics, Spain) electrodes were placed over Cz. We selected the F3 (F4 when monitoring the right hemisphere) anodal and Cz cathodal tDCS montage based on computational modeling (using StimViewer, Neuroelectrics, Spain) in order to target primarily the outer convex brain territory (superficial divisions) of the middle cerebral artery (MCA).

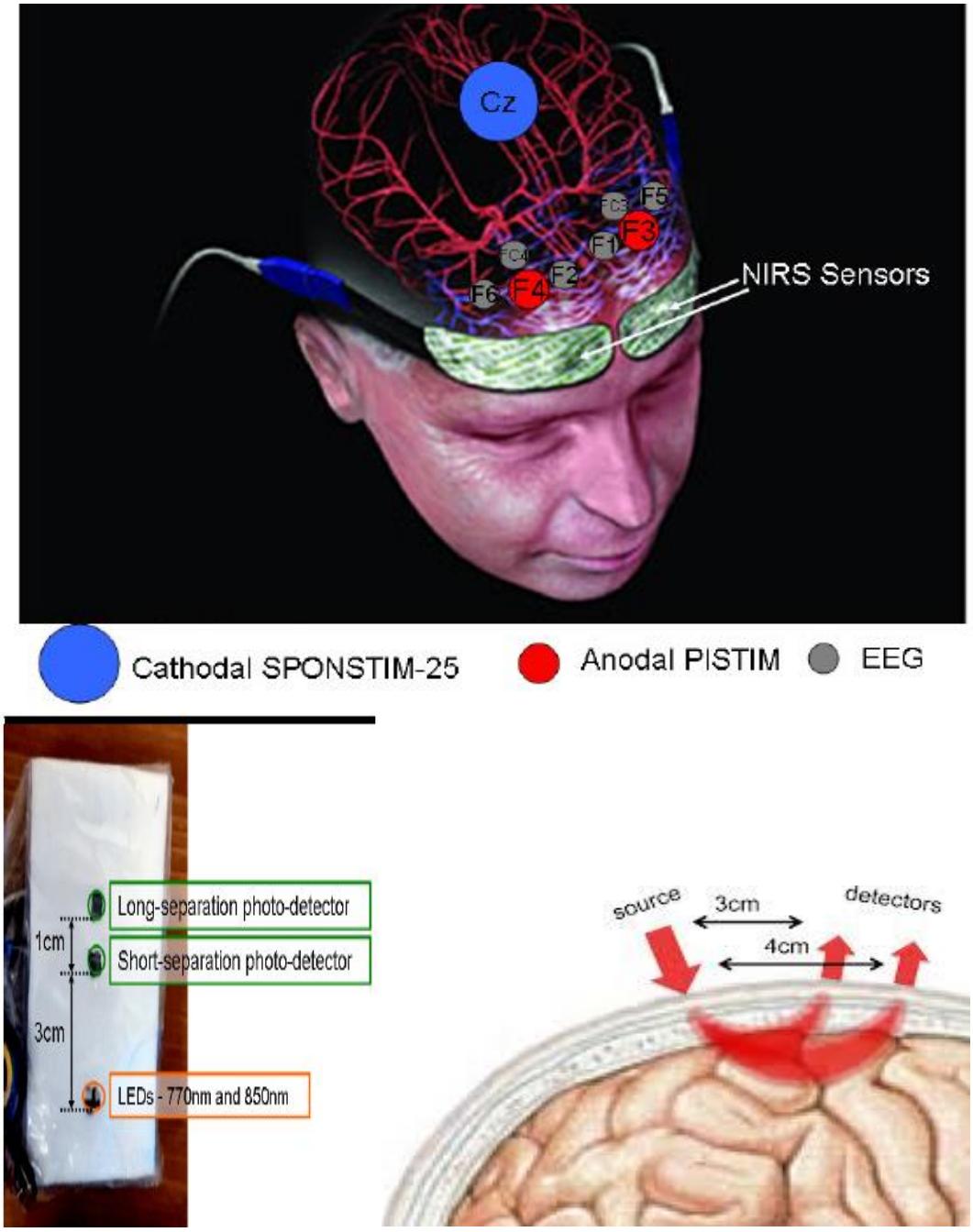

Fig 3.1 (a) NIRS-EEG/tDCS joint-imaging montage

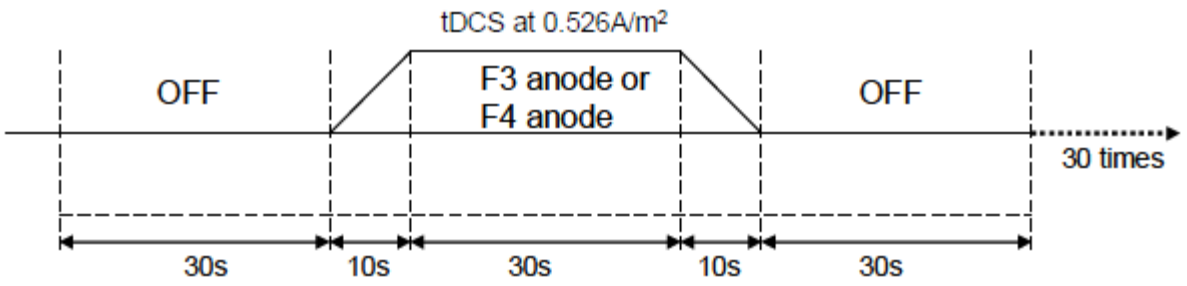

Fig 3.1 (b) tDCS protocol

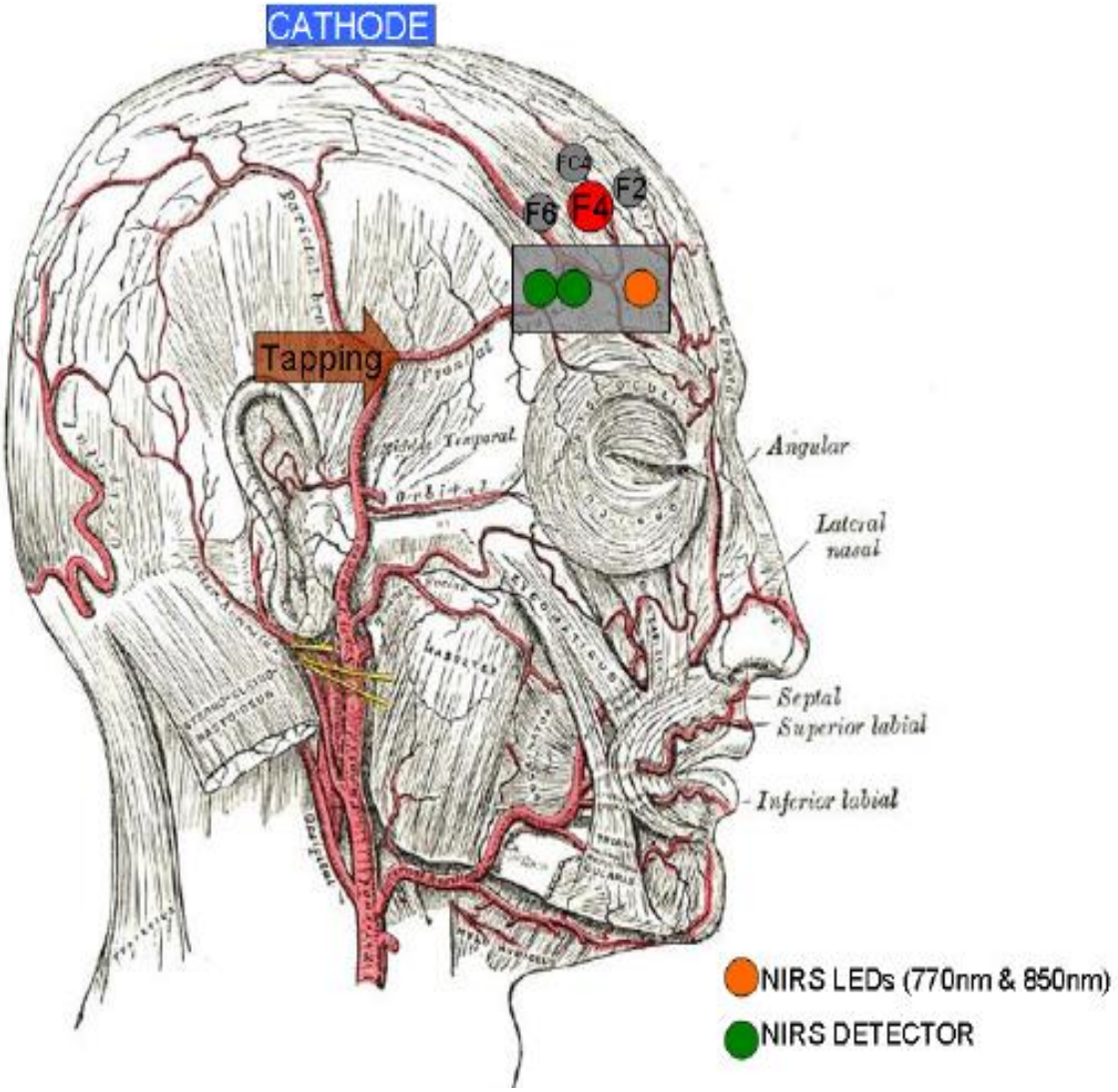

Fig 3.1 (c) Digital tapping of anterior temporal artery

MCA is one of the three major paired arteries that supply blood to the cerebrum and is the most commonly occluded vessel in ischemic stroke. The tDCS at a current density of 0.526A/m2 was turned ON for 30sec with 10sec ramp-up and ramp-down (see Fig 3.1(b)), which was repeated 15 times in random order with 30sec OFF periods in between for the lesioned and contra-lesioned hemispheres (ischemic stroke was restricted to a single hemisphere). Using our own custom-built hardware, we conducted the eyes-open block-averaged resting-state NIRS oximeter measurements [37] just above each eyebrow at the F3 and F4 sites using a custom-built NIRS sensor (see Fig 3.1(c)) that is similar in design to SomaSensor (SAFB-SM, INVOS, USA). The custom-built NIRS sensor consists of two LED sources (770nm and 850nm) and two photodiode detectors at a distance of 3 cm and 4 cm so that the short separation NIRS signal can be regressed out from the longer separation NIRS signal in order to diminish the systemic interference [37]. Also, the eyes-open resting state EEG (StarStim, Neuroelectrics, Spain) is recorded at 500Hz from the nearby electrodes F1, FC3, F5, F2, FC4, F6 (international 10-20 system).

3.2 Temporal artery tap technique to identify systemic interference using short separation NIRS measurements

The frontal branch of the superficial temporal artery (anterior temporal) runs forward to the forehead and can be manually tapped lightly to create fluctuations in the blood supply to the forehead (see Figure 3.1(c)). This fluctuations should be registered primarily by the short separation NIRS signal where the longer separation NIRS signal can be considered contaminated [37] with a filtered version of the short separation NIRS signal. This short separation NIRS signal to artefact filter can be found by least-square fitting the recorded fluctuations in the short separation NIRS signal during temporal artery tap to the longer separation NIRS signal in resting-state without tDCS. The temporal artery tap should produce large (compared to baseline NIRS signals) impulse-like fluctuations which should make the least square fitting easier to find the impulse response. The systemic interference can then be found by convolving any short separation NIRS signal with the impulse response, and then subtracting that from the respective longer separation NIRS signal.

3.3 NIRS-EEG/tDCS joint-imaging data analysis with and without temporal artery tap technique

We pre-processed the EEG data using EEGLAB functions [38] and then averaged the log-transformed mean-power of EEG within 0.5Hz-11.25Hz range (selected based on earlier work [39]) from F3, F1, FC3, F5 sites for left hemisphere and from the F4, F2, FC4, F6 sites for the right hemisphere. The percent change in log transformed mean-power of EEG within 0.5Hz-11.25Hz frequency band is computed for the first 10 sec of ON periods (called "initial dip" in our

prior work [39]) relative to the first 10 sec of OFF periods. The percent change in log transformed mean-power of EEG within 0.5Hz-11.25Hz frequency band is analyzed for both the lesioned and contra-lesioned hemispheres. Eyes-open block-averaged resting-state percent change in the mean regional cerebral hemoglobin oxygen saturation (rSO2) in the first 10 sec of ON periods (called "initial dip" in our prior work [39]) relative to the first 10 sec of OFF periods is measured from the NIRS signals where the Baseline is set at the start of the experiment. In one case (rSO2subtract), the short separation NIRS signal is subtracted from the longer separation NIRS signal while for the other case (rSO2filter), the short separation NIRS signal is convolved with the impulse response and then subtracted from the respective longer separation NIRS signal.

3.4 Results

We observed that there was an increase in log-transformed mean-power of EEG within 0.5Hz-11.25Hz frequency band in the first 10 sec of ON periods relative to the first 10 sec of OFF periods for the contra-lesioned hemisphere stimulation/recording. This increase is primarily in the Theta (4–8 Hz) frequency band in agreement to our prior results [39]. Also, there is a corresponding decrease in the mean rSO2subtract in the first 10 sec of ON periods (called "initial dip" in our prior work [39]) relative to the first 10 sec of OFF periods where the individual Baseline for rSO2subtract measurements is set at the beginning of the session.

. The "initial dip" is found to be greater for the lesioned hemisphere stimulation/recording where the percent change in the mean rSO2subtract mostly correlated with the corresponding percent change in log-transformed mean-power of EEG within 0.5Hz-11.25Hz frequency band. Interestingly, the percent change in the mean rSO2filter for the lesioned hemisphere better correlates with the log transformed mean-power of EEG within 0.5Hz-11.25Hz frequency band as shown in Table 3.2.

3.5 Discussion

In this study, we found that the percent change in the mean rSO2 typically correlated with the corresponding percent change in log-transformed mean-power of EEG within 0.5Hz-11.25Hz frequency band. We also found in the contra-lesioned hemisphere of the stroke survivors that there is an immediate increase in the 0.5Hz-11.25Hz frequency band during anodal tDCS [39]; however, there is also significant inter-subject variability after tDCS. Here, the percent change in the mean rSO2filter for the lesioned hemisphere better correlates with the log-transformed mean power of EEG within 0.5Hz-11.25Hz frequency band than the percent change in the mean rSO2subtract. Of note, we found in some stroke subjects interhemispheric laterality in the systemic interference as well as rSO2filter evoked by anodal tDCS. Indeed, Large Artery Atherothrombosis leads commonly to stenosis at the bifurcation of the carotid artery (carotid stenosis). At the bifurcation of the carotid artery arises the internal carotid artery (ICA) that supplies blood to the brain as well

Table 3.2 Results

Case	**Post-tDCS (mean±1 std. dev.)**	
	Correlation Coefficient with $rSO2_{subtract}$	Correlation Coefficient with $rSO2_{filter}$
1	0.42 +/- 0.18	0.54 +/- 0.12
2	0.49 +/- 0.14	0.58 +/- 0.14
3	0.54 +/- 0.17	0.61 +/- 0.12
4	0.48 +/- 0.14	0.57 +/- 0.15
5	0.53 +/- 0.18	0.59 +/- 0.13

as the external carotid artery (ECA) that supplies blood to the head and neck, such as face, scalp, etc. Inter-hemispheric laterality of carotid stenosis may lead to laterality in the hemodynamic response to tDCS both at the brain (due to ICA) as well as the superficial layers (due to ECA). Since ischemic stroke secondary to carotid stenosis is common in older people so our preliminary studies showed the feasibility of identifying the lesioned hemisphere in subacute ischemic stroke with the low-cost NIRS-tDCS hardware [25]. Indeed, prior cross sectional studies suggest that impaired cerebral hemodynamics precedes stroke where cerebrovascular reactivity (CVR) reflects the capacity of blood vessels to dilate, and is an important marker for brain vascular reserve [40]. CVR provides an useful addition to the traditional baseline blood flow measurement where severely reduced CVR predicts the risk of ipsilateral ischemic stroke and TIA [40] as well as mild cognitive impairment [41] and vascular dementia [42]. A meta-analysis summarizing the association between CVR impairment with stroke risk demonstrated a 4-fold higher stroke risk in asymptomatic patients with impaired cerebral blood flow [42]. However, the cost, access, and availability of trained technicians and physicians to perform the Transcranial Doppler (TCD) blood flow velocity measurements of CVR in a community setting is one of the main limitations [43].

It cannot be excluded that in certain stroke survivors the lesioned hemisphere may not respond to anodal tDCS with an increase in neural activity. This may result in an absent change in the cerebral metabolic rate of oxygen, CMRO2 (i.e., oxygen consumption) [44] that is defined as the difference of oxygen flow into and out of the tissue, as compared to the non-lesioned hemisphere. To avoid

this potential problem, the effects of tDCS on neural activity can be elucidated with simultaneous EEG, which provides an independent measure to supplement NIRS recordings. Based on prior work [45] that found an association of individual resting state EEG alpha frequency and cerebral blood flow, we hypothesize that if the changes in EEG during tDCS are correlated with the changes in NIRS, then this may enable us to measure the state of neurovascular coupling. Moreover, with the anterior temporal artery tap technique, we may be able to classify carotid stenosis, ECA stenosis, and ICA stenosis patients based on the laterality in the hemodynamic response to tDCS both at the brain (due to ICA) as well as at the superficial layers (due to ECA), e.g., ICA stenosis vs. ECA stenosis based on the laterality in the rSO2filter vs. in the systemic interference evoked with anodal tDCS. If verified by future prospective multicenter trials, these findings may have important implications for both prognosis and rehabilitation of stroke survivors.

In next two chapters, Effects of transcranial direct current stimulation (tDCS) from simultaneous recording of electroencephalogram (EEG) and near infrared spectroscopy (NIRS) are presented. Here, tDCS has been shown to modulate cortical neural activity leading to changes in the EEG power spectrum. At the time of any neural activity, the electric currents from excitable membranes of brain tissue generate a potential at a given location closely relating to the cerebral blood flow (CBF) that supplies glucose via neurovascular coupling. CBF is increased in brain regions with neural enhanced activity via metabolic coupling mechanisms. An ARX model is developed for online parameter estimation with a Kalman Filter to capture the online tracking of tDCS neuro-modulatory effects.

Chapter 4
Online tracking of NIRS EEG during tDCS parameter estimation with an Autoregressive model

The preliminary studies have shown that anodal tDCS increases regional cerebral blood flow [46] and evokes neuronal and hemodynamic responses (oxy-hemoglobin (oxy-Hb) and deoxy-hemoglobin (deoxy-Hb)) in the brain tissue [47]. During electrical modulation of the brain tissue, the electric currents from excitable membranes superimpose at a given location in the extracellular medium and generate a potential which can be recorded as electroencephalogram (EEG) from scalp. Among the different brain imaging techniques, EEG is considered to have an excellent temporal resolution (on the order of milliseconds) and reasonable spatial resolution (~1 cm) [2]. The respective neural activity requires supply of oxygen and glucose via neurovascular coupling which therefore closely relate, spatially and temporally, to the regional hemodynamic response [48]. Besides neurovascular coupling, tDCS can have direct effect on the smooth muscle of blood vessels where cerebral autoregulation mechanisms can ensure that the blood flow is maintained during changes of perfusion pressure. Functional near-infrared spectroscopy (fNIRS) allows us to monitor the regional hemodynamic response noninvasively with reasonable spatial (~1 cm) and excellent temporal (milliseconds) resolution [49].

Furthermore, anodal HD-tDCS induced modulation of cortical sensorimotor networks using fNIRS has been shown recently [50] where the fundamental relationship between local changes in cerebral hemodynamics and the underlying neural activity during tDCS remains largely unknown [51]. In a study by Dutta et al., a phenomological model has been presented that captures the capacity of blood vessels to dilate during anodal tDCS due to neuronal activity, causing increased demands of energy where tDCS can modulate the coupling between the oxy-Hb time-series and log-transformed mean-power time-course of EEG [51]. Indeed, slow (0.07-0.13 Hz) hemodynamic oscillations during awake rest can be temporarily (duration ~100 sec) coupled with EEG (alpha and/or beta power) power fluctuations in sensorimotor areas and modulate the excitability level in the brains' motor areas [53]. Also, Nikulin et al [54] showed monochromatic ultra-slow oscillations (MUSO) around 0.1 Hz in the EEG signals, their relation to the oxy-Hb fNIRS signals, and hypothesized that EEG MUSO represents an electric counterpart of the hemodynamic responses. However, online tracking of the relation between EEG and fNIRS data acquired simultaneously from the human cortex during tDCS has not been investigated. In this chapter, a computational autoregressive (ARX) model is developed for online parameter estimation with a Kalman filter to track transient coupling relation between EEG band (0.5-11.25 Hz) power and oxy-Hb NIRS signals acquired simultaneously from the human sensorimotor cortex during anodal HD-tDCS.

In the first section of this chapter, we explain the basics of EEG analysis (frequency bands and band-power measurement). The second section discusses the relationship between EEG band power and cerebral hemodynamic oscillations at low frequency based on prior works. In further sections, we discuss the ARX model and Kalman Filter.

4.1 Electroencephalography (EEG)

EEG is the most studied non-invasive brain machine interface, mainly due to its fine temporal resolutions, ease of use, portability and low set-up cost [54]. Electric currents from excitable membranes of brain tissue superimpose at a given location in the extracellular medium and generate a potential, which is referred to as the electroencephalogram (EEG) when recorded from scalp [55]. In clinical context, EEG refers to the continuous recording of the brain's spontaneous electrical activity over a period of time, as recorded from multiple electrodes placed on the scalp. Diagnostic applications generally focus on the spectral content of EEG, that is, the different spectral bands of neural oscillations that can be observed in EEG signals [56]. Despite limited spatial resolution, EEG continues to be a valuable tool for research and diagnosis, especially when millisecond-range temporal resolution (not possible with CT or MRI) is required. It is the most direct correlate of online brain processing that is obtainable non-invasively [56].

4.1.1 Estimating neural activity from EEG

The EEG is typically described in terms of [31] [57]

- Rhythmic Activity
- Transients

The rhythmic activity is divided into bands by frequency based on their spectral content. To some degree, these frequency bands are a matter of nomenclature (i.e., any rhythmic activity between 8–12 Hz can be described as "alpha"), but these designations arose because rhythmic activity within a certain frequency range was noted to have a certain distribution over the scalp or a certain biological significance. Frequency bands are usually extracted using spectral methods (for instance, Welch's power spectral density estimates; [58] as implemented for instance in freely available EEG software such as EEGLAB [48] or the Neurophysiological Biomarker Toolbox [58], besides others.

4.1.2 EEG frequency bands

EEG power spectrum mostly falls within the range of 1–20 Hz where activity below or above this range is likely to be artefactual under standard clinical recording techniques. Nevertheless, EEG power spectrum is broadly divided up to 100Hz for quantitative EEG (QEEG) analysis which is then subdivided in frequency bands called alpha, beta, theta, delta, etc. based on the major EEG bandwidth used in clinical practice [59][60]. The EEG frequency bands used for QEEG analysis in clinical practice follows:

1. Alpha Band:
It is the frequency range from 7 Hz to 14Hz. It is the first rhythmic activity seen by Hans Berger [61]. It is seen primarily in the posterior regions of the head on both sides and higher in amplitude

on the dominant side. The posterior basic rhythm emerges with closing of the eyes and with relaxation, and attenuates with opening of the eye and mental exertion. The alpha activity in the contralateral sensory and motor cortical areas is called the mu rhythm that emerges when the hands and arms are idle. When the alpha becomes abnormal, the person is not even responsive to external stimuli.

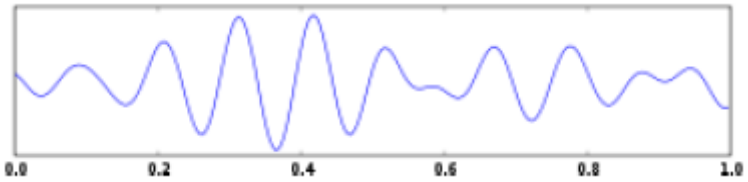

Fig 4.1 EEG Alpha Band

2. Beta Band:

It is the frequency range from 15Hz to 30 Hz. It may be absent or reduced in areas of cortical damage [61]. It is the dominant rhythm in patients who are alert or anxious or who have their eyes open.

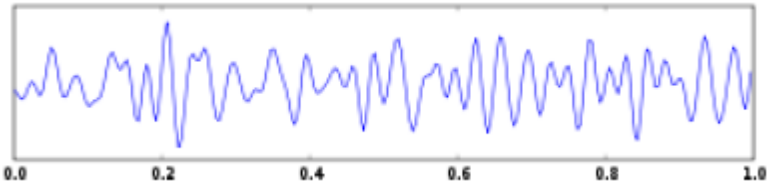

Fig 4.2 EEG Beta Band

3. Delta Band:

It is the frequency range up to 4 Hz. It tends to be the highest in amplitude and the slowest wave. It may occur focally with subcortical lesions and in general distribution with diffuse lesions and deep midline lesions [61]. It is found most prominent in frontal region in adults and posterior in children.

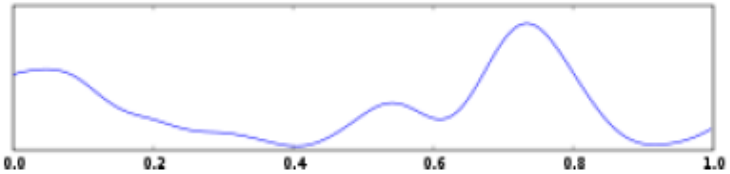

Fig 4.3 EEG Delta Band

4. Theta Band:

It is the frequency range from 4Hz to 7 Hz. It can be seen as a focal disturbance in focal sub-cortical lesions [61].

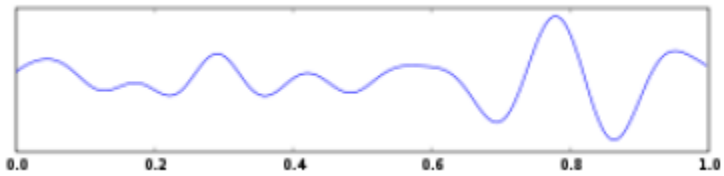

Fig 4.4 EEG Theta Band

5. Gamma Band:
It is the frequency range approximately 30-100 Hz. Gamma rhythms represent binding of different populations of neurons together into a network for purpose of carrying out a certain motor or cognitive function [61].

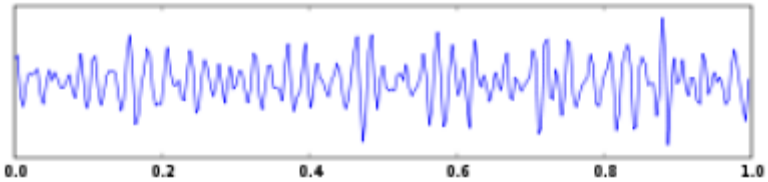

Fig 4.5 EEG Gamma Band

4.2 Oscillations in EEG band power and brain hemodynamics

Prior works have shown a relationship between human electroencephalogram and hemodynamics based on fNIRS and EEG [62]. Also, modelling studies (see Fig. 4.6) have shown how neurons can convey "hunger" signals to the vascular network via an intervening layer of glial cells (astrocytes); vessels dilate and release glucose which fuels neuronal firing [63]. In principal accordance, in this study, we especially investigated slow hemodynamic oscillations around 0.1Hz that can be related to known biological phenomena, i.e., arterial blood pressure, cerebral and skin vasomotion, respiration and neuronal activity [64]. Indeed, hemodynamic activity recorded with NIRS shows pronounced oscillations at 0.1 Hz which are also present in fluctuations of arterial blood pressure, and are called Mayer waves [65]. Here, recent analysis of the various transfer functions of the rat baroreceptor reflex suggests that Mayer waves are transient oscillatory responses to hemodynamic perturbations rather than true feedback oscillations [65]. We specifically investigated the relation of these slow hemodynamic oscillations around 0.1Hz with EEG band power <12Hz to elucidate its neurovascular coupling related aspects due to tDCS perturbations [66]. In the next two sections, a computational autoregressive (ARX) model is investigated using online parameter estimation with a Kalman filter where prior work has shown the feasibility of a Kalman estimator- and general linear model based on-line brain activation mapping by near-infrared spectroscopy [67].

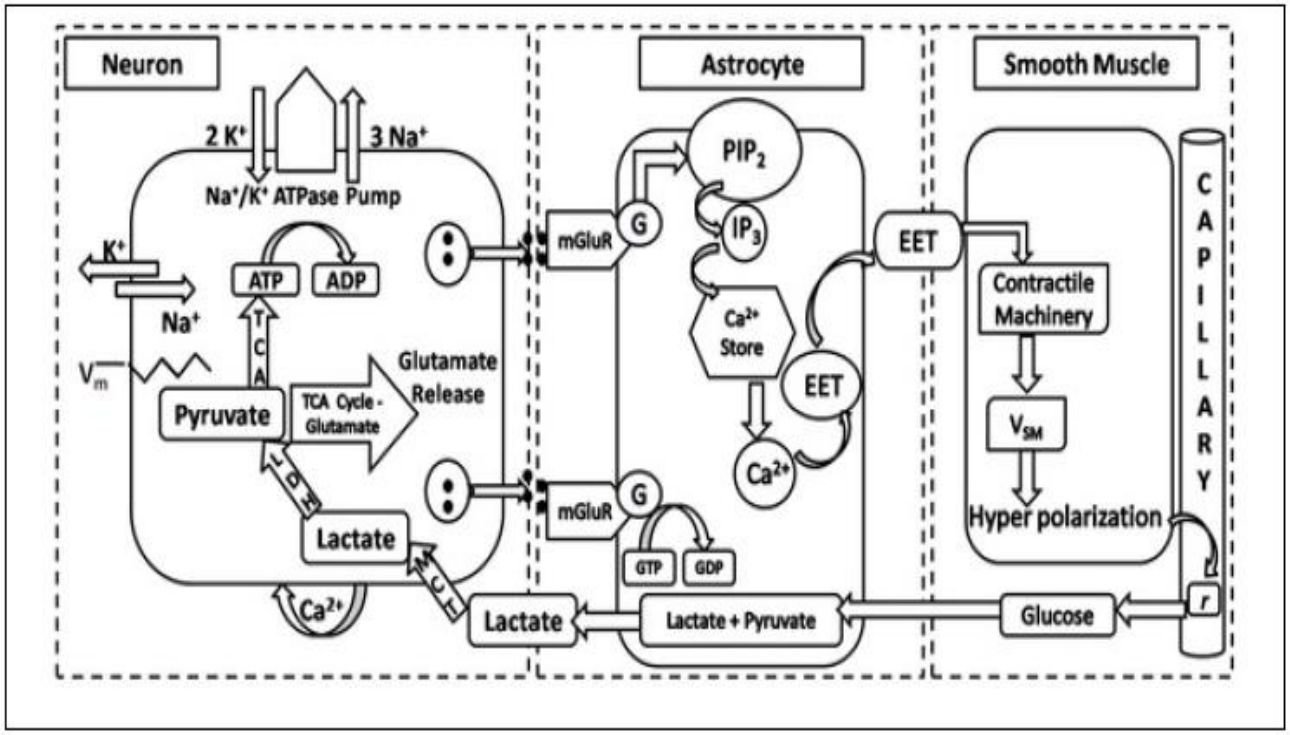

Fig 4.6 Neurons convey "hunger" signals to the vascular network via an intervening layer of glial cells (astrocytes); vessels dilate and release glucose which fuels neuronal firing [23]

4.3 ARX model

There are various methods that can be used to assess the degree of similarity or shared information between two signals. Some of these methods depend on the type of presumptive system which processes the one "input" signal into the other "output" signal. For linear memoryless systems, cross correlation in time domain is used. For linear systems with memory, common methods include autoregressive models with exogenous (that are determined by factors outside of the model) input (ARX), autoregressive moving average (ARMA) etc.
Complex systems such as brain are difficult to analyze because of the huge number of individual neuronal/synaptic paths between nuclei, the nonlinear and non-stationary nature of neuronal connections, and the operation at multiple time scales. One approach is to use simple low order linear models to approximate the transfer function relationship, such as autoregressive with exogenous (ARX) models. Autoregressive is a stochastic process used in statistical calculations in which future values are estimated based on a weighted sum of past values. An autoregressive process operates under the premise that past values have an effect on current values. The advantage of using linear ARX model is that there is no need to estimate non linearity, and less training data is required. However, the performance of such models depends on model order, scale and pre-filtering.

In this study, we adapt and apply the ARX model approach to evaluate the degree of correlation between cortical EEG and oxy hemoglobin dynamics at low frequency oscillations. The ARX

model is a common method to represent output signals from an unknown system by using a linear combination of past output signal values and past input values.

4.3.1 ARX model Structure

The linear time variant system can be described by an autoregressive model with exogenous input (ARX) [68]

$$A(z)y(t) = B(z)\,u(t) + e(t) \tag{1}$$

with transfer function $G(z) = {B(z)}/{A(z)}$

$$A(z) = 1 + a_1 z^{-1} + a_2 z^{-2} \ldots\ldots\ldots\ldots\ldots\ldots + a_l z^{-l}$$
$$B(z) = b_1 z^{-n} + b_2 z^{-(1+n)} \ldots\ldots\ldots\ldots\ldots\ldots + b_m z^{-(n+m-1)} \tag{2}$$

In equation (1), y(*t*) is the output and u(t) is the input at any discrete-time instant t. The z^{-1} is backward shift operator and z^{-1} y(*t*) is equivalent to y (*t −1*) . Also, e(*t*) is the zero mean Gaussian white noise affecting the system. The model has (*l + m + 1*) parameters/coefficients in total i.e. ($a_1 \ldots . a_l$, $b_1 \ldots\ldots b_m$, *n*) where *l* is the number of poles, *m* is the number of zeros plus 1, and *n* is the number of input samples that occur before the input affects the output, also called the dead time in the system. Substituting equation (2) in (1), and expanding, the output of the ARX model can be parameterized as

$$y(t,\theta) = \sum_{i=1}^{l} a_i\, y(t-i) + \sum_{j=1}^{m} b_j\, u(t-j-n+1) + e(t) \tag{3}$$

where $\theta = [a_1 \ldots . a_l , b_1 \ldots . . b_m]^T$ and the size of θ depends on the complexity of the model. Thus, the selection of model order (*l,m,n*) and structure becomes a crucial step in the estimation of unknown parameters in θ.

The system identification toolbox in Matlab (The MathWorks Inc., USA) was used to find an optimal model order and structure (*l,m,n*). The pre-tDCS recording with EEG power as input and NIRS oxy-Hb signal as output provided the estimate of the model order and structure (*l, m, n*). A range of ARX polynomial models were investigated (Fig 4.7) for all the subjects and the "simpler" model (*l=4, m=5, n=5*) in terms of model order that gave comparable unexplained output variance (in %) to the "best" model for all the subjects was selected. Here, elements of θ are time varying as it relates the variations in EEG power to NIRS response. At a given time *t*, the model estimates are predicted using equation (3), assuming that the system is stationary (or slowly time varying during awake rest [53]) during the prediction horizon.

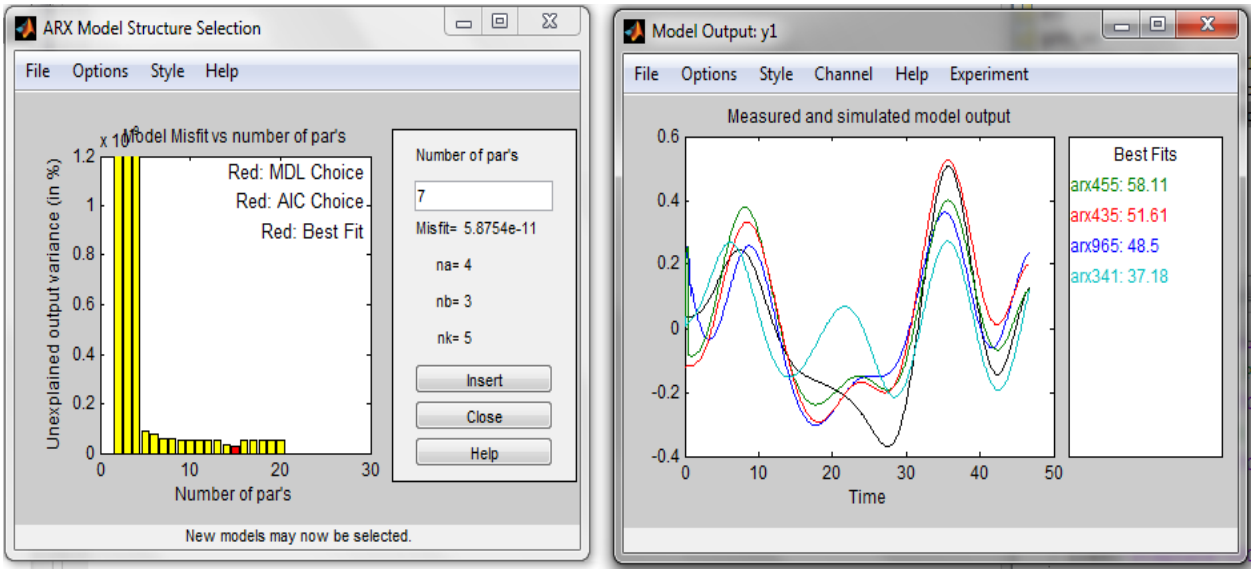

Fig 4.7 The system identification toolbox in Matlab (The MathWorks Inc., USA) was used to find an optimal ARX Model Structure

4.3.2 State Space Representation of ARX model

State space representation of the ARX model is required for the Kalman filter (described in next section) implementation [68] where we considered an ARX (*l*,*m*) model without the dead time since dead time was assumed constant and not estimated. The space state form was:

Process Equation

$$x_k = Ax_{k-1} + Bu_{k-1} \quad (4)$$

Measurement Equation

$$y_k = Cx_k \quad (5)$$

where k represents the current time step. In equation (4), the state vector at the current time step $x_k = [x_1 \ldots\ldots\ldots x_q]^T$, $q = \max\{l, m\}$ and u_{k-1} is the model input at the previous time step. $A \in \mathbb{R}^{(q\times q)}$ matrix relates the state vector at previous time step x_{k-1}, to that of current time step x_k. $B \in \mathbb{R}^{(q\times 1)}$ matrix relates the model input at the previous time step u_{k-1} to the state vector at the current time step x_k. The measurement of the system output at the current time step is given by y_k. $C \in \mathbb{R}^{(1\times q)}$ matrix relates the state vector at the current time step x_k to the measurement at the current time step y_k .Here *A, B, C* may change with each time step of iteration, but in this study we assumed them constant for simplification.

4.4 Kalman Filter

Kalman filter has been named after one of its developer Rudolf E. Kalman. It is a linear, discrete time, finite dimensional time varying system that evaluates the state estimate that minimizes the mean square error. It is recursive in nature and can efficiently estimate the internal states and parameters of a discrete time system from a series of noisy measurements.

A system is driven by an input/set of inputs and its output is evaluated by measurements from sensors/devices such that the knowledge on the system's behavior is solely dependent on the input and the observed output. The observations are often corrupted with errors and uncertainties in the process. Thus, it is required to obtain an estimate of the system's state based on available information that optimizes a given criteria. The Kalman filter is known to be used for the estimation of the unknown state.

The Kalman Filter is an efficient filter, which consists of mathematical equations that implement a predictor-corrector type estimator that is optimal in the sense that it minimizes the estimated error covariance, when some conditions are met. The algorithm works in two steps:

Prediction Step: In this step, the filter produces estimates of the current state variables, with uncertainties involved.

Correction Step: In this step, the outcome of next measurement is observed and the estimates are updated using weighted average method, where more weight is given to estimates with higher certainty.

Thus, the algorithm runs in real time, as it uses only the present input measurements and previously calculated state and its uncertainty matrix, no additional past information is needed.

4.4.1 Kalman filter for ARX online parameter estimation

Here, the coefficients relating the past measurements of NIRS oxy-Hb signal as output and past measurements of EEG power as input are the model parameters that are to be identified. Therefore, the state vector, x, was augmented with the unknown model parameters θ, that are to be identified. Here, by regarding the unknown model parameters as elements of the state vector, the basic Kalman filter algorithm was followed for the estimation of the state vector as well as the model parameters. Consequently, the meta state vector $w_k = [x_k ; \theta_k]^T$, was created for the basic Kalman filter algorithm where k indicates the current time step. The model parameters in θ were assumed to be locally time-invariant when compared to the process. Consequently, the augmented Kalman filter system was given by,

Process Equation

$$w_k = F(w_{k-1}, u_{k-1}) \quad (6)$$

where $F(w_{k-1}, u_{k-1}) = \lfloor f(x_{k-1}, u_{k-1}) ; \theta_{k-1} \rfloor$

Measurement Equation

$$y_k = H\, w_k \tag{7}$$

where $H = \begin{bmatrix} C & 0^{1\,X\,(l+m)} \end{bmatrix}$

Now, the recursive estimation of the state space model can be performed using the prediction and correction steps of the basic Kalman filter algorithm where,

Prediction Step

At step *k*, the a priori estimate of the state w'_k is given by the a posteriori state at previous step, w'_{k-1}.

$$w'_k = F(w'_{k-1}\ u_{k-1}) \tag{8}$$

$$P'_k = D_k P_{k-1} D_k^T + Q_{k-1} \tag{9}$$

P_k is the estimated error covariance, Q_k is a process noise covariance diagonal matrix, and D_k is the process jacobian with respect to variables involved.

$$D_{[i,j]} = \frac{\partial F_{[i]}}{\partial w_{[j]}}\left(\hat{w}_{k-1},\ u_{k-1}\right)$$

Correction Step

K_k is called Kalman Filter gain, R_k is a scalar measurement noise covariance.

$$K_k = P'_k\, H_k^T\, (H_k\, P'_k\, H_k^T + R_k)^{-1} \tag{10}$$

The updated state w_k and updated estimate error covariance P_k is computed as follows:

$$w_k = w'_k + K_k(y_k - H_k\, w'_k \tag{11}$$

$$P_k = (1 - K_k\, H_k)\, P'_k \tag{12}$$

Here, in the equation (8) of the prediction step, the a priori estimate of the meta-state vector at the current time step w'_k , is given by the process equation (6) using the a posteriori estimate of the meta-state vector at the previous time step, w'_{k-1}.

The limitation in the approach is the degradation of Kalman Filter's performance in estimating time varying parameters as it refers to the entire history of past measurements. Since tDCS may lead to transients in NIRS oxy-Hb signal, therefore tracking of this becomes important with the model parameters.

In order to track this time varying nature, a forgetting factor lambda λ is introduced [69].

$$P'_k = \frac{D_k P_{k-1} D_k^T}{\lambda} \quad (13)$$

$$K_k = P'_k H_k^T (H_k P'_k H_k^T + \lambda)^{-1} \quad (14)$$

The forgetting factor is closer to 1 means that the filter will forget fewer past measurements. A trade-off between the smoothness of tracking and lag in detecting the changes in model parameters should be considered when forgetting factor is introduced to a Kalman filter. Usually $\lambda \in [0.9, 1]$ is suitable for most application.

4.5 Validation of Time-Varying ARX Model Estimation with Kalman Filter

The elements of the meta state vector wk = [xk ; θk], were initialized as zero. The initial output estimate as also set to zero. The estimate of the error covariance was initialized to identity matrix, Po = I. In simulation, the invariant parameter tracking as evaluated first with the Kalman filter to investigate the stability of the model. Then, in order to investigate Kalman filter's robustness to the time varying phenomenon, the model parameters ere solely changed to simulate tracking of time varying properties of nonstationary signals. The advantage of simulation is that true parameters are known and therefore can be compared with the estimated ones. The ARX model structure as chosen to l=3, m=3, n=1 for simulations. Thus, six parameters, θ = [a1, a2, a3, b1, b2, b3], were estimated via the Kalman filter algorithm in simulation. Here, pseudo random binary sequence was chosen as the model input [68]. The corresponding parameter estimates of the model are also shown in Fig 4.8. The solid lines and dotted lines represent true parameters and estimated parameters from the model respectively. As the model parameters vary gradually, the estimates track the changes well which implies that the estimation method is suitable for time variant parameter tracking with an ARX model.

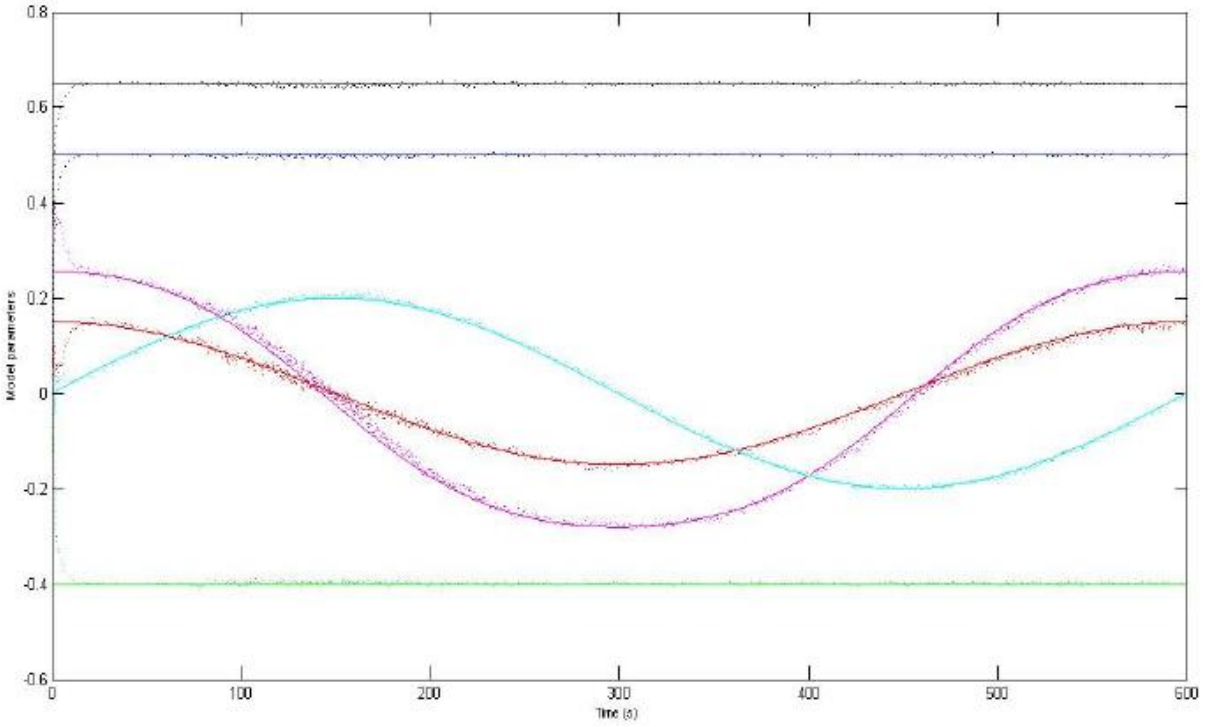

Fig 4.8 True parameters represented by bold lines, estimated parameters represented by dotted Lines

Table 4.1 Parameter Estimates

Parameters	MAE	RMSE	Std
a1	0.0080	0.0152	0.0130
a2	0.0066	0.0124	0.0105
a3	0.0044	0.0057	0.0036
b1	0.0031	0.0187	0.0185
b2	0.0034	0.0177	0.0174
b3	0.0035	0.0207	0.0204

The mean absolute error (MAE), normalized root mean squared error (RMSE), and the standard deviations (Std) of the parameter estimates (with respect to the true parameters) were estimated and shown in Table 4.1. This scheme was based on a class of time-varying Auto Regressive with an exogenous input (ARX) model where the associated time-varying parameters are represented by multi-wavelet basis functions. The orthogonal least square (OLS) algorithm is then applied to refine the model parameter estimates of the time-varying ARX model.

4.6 Discussion

Following validation using simulated signals, the time-varying ARX model estimation with Kalman filter was applied on human data and the online tracking results were compared with that from conventional sliding window cross correlation calculations [53]. Here, a moving window size of 100sec with an overlap of 0.1 second and the number of lag of ±20sec (Matlab function 'crosscorr') was selected based on prior work [53] which identified short-lasting coupling of duration ~100sec with lead/lag. The next chapter discusses the experimental protocol followed for online tracking of tDCS using NIRS – EEG joint imaging in healthy subjects followed by the results obtained from the experiment.

Chapter 5

Investigating Online Effects of tDCS from NIRS –EEG joint imaging

In the previous chapter, a computational autoregressive (ARX) model was developed for online parameter estimation with a Kalman filter to track transient coupling relation between EEG band (0.5 11.25 Hz) power and oxy-Hb NIRS signals acquired simultaneously from the human sensorimotor cortex during anodal HD-tDCS. This chapter discusses the application of online parameter estimation technique on healthy subjects and it is shown to be sensitive towards transient changes in the cross correlation between EEG band power and oxy –Hb fNIRS signals in the low frequency (< 0.1 Hz) regime. Compared to conventional sliding window fNIRS-EEG cross correlation calculations, this method allows quantitative assessment of the transient coupling relationship between electrophysiological and hemodynamic response to HD-tDCS, which could be used to monitor the tDCSs' neuro-modulatory effect in health and disease.

5.1 Methods

5.1.1 Subjects

We conducted experiments on five healthy subjects (23-42 years) who volunteered to participate in this study after informed consent, and all experiments were conducted in accordance with the Declaration of Helsinki. The subjects had no known neurological or psychiatric history, nor any contraindications to tDCS. During the experiment, the subjects were well seated in an armchair with adjustable height and angle in front of a table.

5.1.2 Experimental Setup

The set-up of HD-tDCS electrodes, EEG, and fNIRS optodes was mounted on the surface of the scalp according to the 10-20 system (see Figure 5.1). The anodal HD-tDCS (StartimR, Neuroelectrics NE, Barcelona, Spain) is in a 4x1 ring configuration with the anode placed in the center (C3) in a region overlying the left primary sensorimotor cortex (SMC), and the return electrodes were placed approximately 4 cm away at FC1, FC5, CP5 and CP1 (see Figure 5.1 and 5.2).

fNIRS: Measurements of changes in oxy-Hb and deoxy-Hb concentrations from the bilateral SMC were made from a 16-channel continuous-wave fNIRS system (Oxymon MkIII, Artinis, Zetten, The Netherlands) at a sampling frequency of 10 Hz. The receiver transmitter distance of 3 cm was chosen, which allowed for a penetration depth of roughly 1.5cm below the scalp. The receivers (Rx) were placed on the FC3 and CP3 for the left hemisphere and FC4 and CP4 for the right hemisphere (Figure 1a). Transmitters (Tx) were placed diagonally, i.e., at P1, P5, C1, C5, F5 and F1 for the left hemisphere and at P6, P2, C6, C2, F2 and F6 for the right hemisphere, as shown in Fig 5.1.

EEG: Twenty-three channels of raw unreferenced (active electrode) EEG signal were recorded (ActiveTwo, Biosemi B.V. Netherlands). EEG artifacts related to tDCS are possible due to electrical

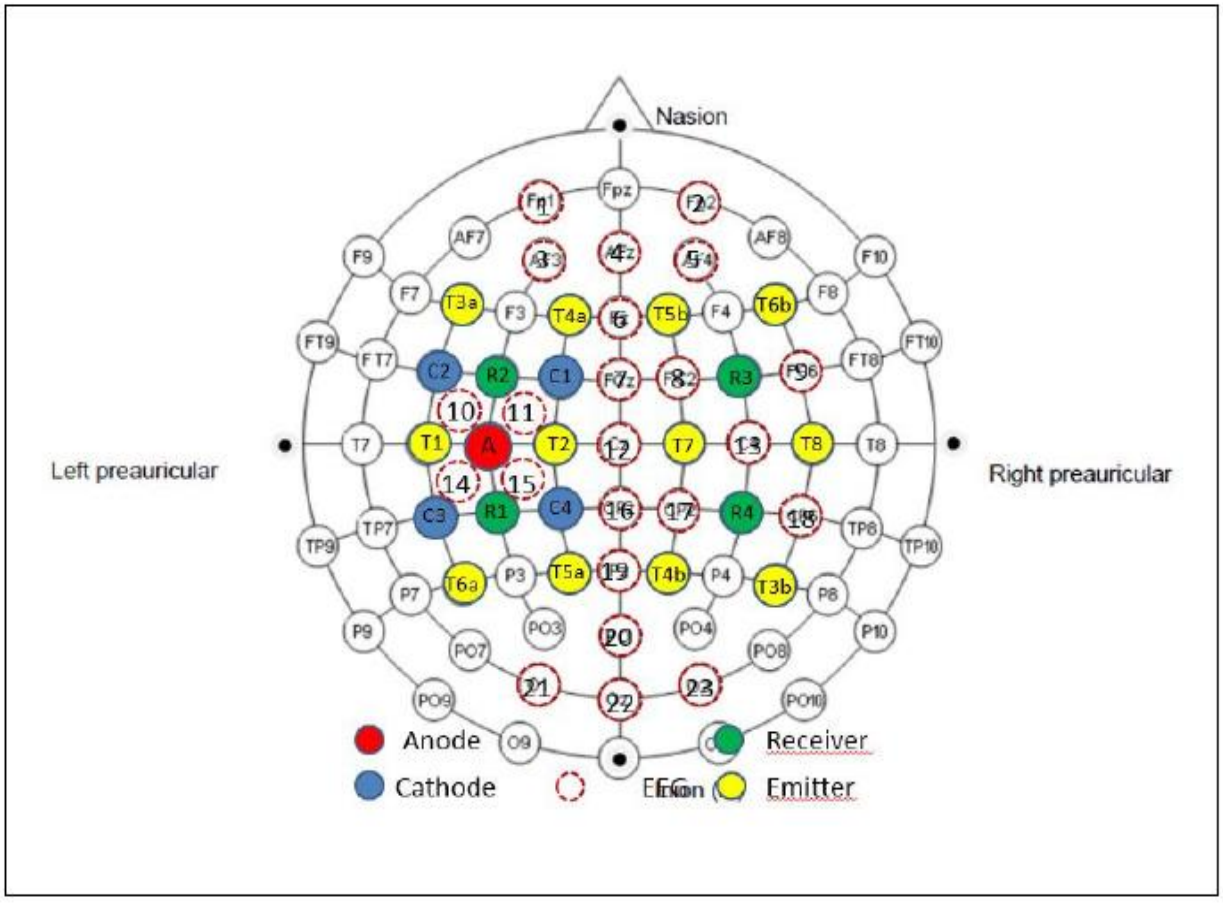

Fig 5.1 Set-up of HD-tDCS electrodes, EEG, and fNIRS optodes in 10-20 system (labeled C1, C2, C3, C4 as cathodes and A as anode).

issues (e.g., unknown electrode impedance changes during stimulation) where concurrent recording is possible with an optimized device (StartimR, Neuroelectrics NE, Barcelona). The twenty three EEG channels included AF3, AFz, AF4, Fz, FCz, FC2, FC6, FCC5h, FCC3h, Cz, C4, CCP5h, CCP3h, CPz, CP2, CP6, Pz, POz, O1, Oz, O2, Fp1, Fp2, as shown in Fig 5.1.

5.1.3 Experimental protocol

As we discussed in previous chapters, Anodal tDCS increases cortical neuronal excitability during the stimulation and for a short-term period after. Due to dispersion in the skull, the spatial resolution of conventional tDCS is reduced significantly. In order to track the neuro-modulatory effects of tDCS using NIRS-EEG based brain imaging, the use of high-definition tDCS (HD-

tDCS) is recommended by neurologists. It constrains the region of modulation between the active electrode and the four surrounding return electrodes (~4cm apart) in a ring montage [11].

Fig 5.2 Illustrative example of the fNIRS-EEG/HD-tDCS set-up (red ellipse) overlying the left primary sensorimotor cortex (SMC).

We divided the experiment into two sessions (pre- and during- HD-tDCS) for the purposes of this computational work. Different sessions were marked by sending markers using TCP/IP to StartimR (Neuroelectrics NE, Barcelona, Spain), and simultaneous acquisition of all the sensor (EEG and fNIRS) signals were TTL-synchronized at Active Two (Biosemi B.V., Netherlands) and Oxymon MkIII (Artinis, Zetten, The Netherlands) using custom-written code in Matlab (Mathworks Inc., USA). Pre-tDCS session had 3 minutes of rest to have a baseline acquisition. During HD-tDCS session, 2mA current was delivered using PISTIM electrodes (Neuroelectrics NE, Barcelona, Spain) with π cm2 (1 cm radius) contact surface. HD-tDCS was delivered for 20 minutes with ramp-up and ramp-down of 30 seconds each. All the synchronized sensor data files were saved and analyzed offline after the completion of the two sessions.

EEG and fNIRS data analysis: The raw unreferenced (active electrodes) EEG data was preprocessed offline using EEGLAB open-source Matlab (Mathworks Inc., USA) toolbox [70], specifically, the data was referenced to ‘average reference' and then artefactual ("non-stereotyped" or "paroxysmal" noise) epochs were removed following visual inspection of the data.

Then, artefact rejection was performed with Independent Component Analysis (ICA) which provides a powerful tool for eliminating several non-brain artifacts from EEG data [70]. Then, log (base-10) transformed mean power of ICA-pruned-EEG data within the 0.5-11.25 Hz range was computed (see Dutta et al [52] for details). The EEG mean-power time-series was down sampled to 10 Hz to match the sampling frequency of the fNIRS oxy-Hb data. Then, the baseline corrected fNIRS oxy-Hb time series as well as the EEG mean-power time-series were 5th order Butterworth zero-phase digital low-pass filtered at 0.1 Hz cut-off frequency to isolate the slow oscillations [53].

5. 2 Results

The simulation of the online time varying ARX model estimation with a Kalman Filter was performed (dicussed in previous chapter). After testing the online parameter estimation with a simulated time-varying ARX model, system identification toolbox in Matlab (The MathWorks Inc., USA) was used to find the best model order from the pre HD-tDCS experimental data where ARX model (l = 4,m =5, n =5) was found to be the simplest model across all the 5 subjects. Therefore, the ARX model (l = 4, m = 5) with 4 poles, 6 zeros, and a constant dead time, n = 5 (in sample periods of 0.1sec), was used for the online tracking of the coupling relationship between EEG band (0.5-11.25Hz) power as input and fNIRS oxy-Hb signal as the output in the slow oscillation regime (< 0.1 Hz). A small (0.5sec) constant dead time meant that we tracked primarily short-duration in phase and out of phase coupling between fNIRS oxy-Hb signal (as output) and EEG band (0.5-11.25 Hz) power signal (as input) which has been shown during awake rest [53]. The variation in the ARX parameters due to change in cross-correlation between EEG band (0.5-11.25 Hz) power and fNIRS oxy-Hb signal was compared with sliding cross correlation calculations [53], as shown with an illustrative example (subject 5) in Figure 1c. The parameters values found for the 5 subjects at the start of HD-tDCS (pre HD-tDCS) and after the end of HD-tDCS session (post HD-tDCS) are given in Table 5.1.

In Figure 5.4 (a), transients in the time-series of zeros were found around 294sec and 428sec which were investigated with the cross correlation function along with its estimation error bounds (shown in Figure 5.4 (b)) that measured the similarity between fNIRS oxy- Hb signal and 20sec shifted (lagged) copies of EEG band (0.5Hz-11.25Hz) power signal within 100sec window centered at 294sec (top panel of Figure 1d) and 428sec (bottom panel of Figure 5.4 (b)). In accordance, Figure 1e shows the short-duration (~100sec) in phase and out of phase coupling between fNIRS oxy-Hb signal and EEG band (0.5-11.25 Hz) power signals around 294sec and 428sec.

Table 5.1 Parameter Values for 5 healthy subjects before and after tDCS

Pre HD –tDCS

Parameters	Subject 1	Subject 2	Subject 3	Subject 4	Subject 5	Mean ± Std. Dev
a1	3.24	3.25	3.24	3.23	3.21	3.23 ± 0.02
a2	-3.73	-3.77	-3.76	-3.74	-3.72	-3.74 ± 0.02
a3	1.78	1.77	1.79	1.72	1.71	1.75 ± 0.04
a4	-0.25	-0.26	-0.25	-0.24	-0.29	-0.26 ± 0.02
b1	0.025	0.018	0.096	0.001	0.270	0.08 ± 0.11
b2	0.016	0.001	0.061	0.664	0.001	0.15 ± 0.29
b3	0.001	0.182	0.001	0.001	0.001	0.04 ± 0.08
b4	0.001	0.147	0.001	0.001	0.001	0.03 ± 0.07
b5	0.001	0.001	0.001	0.001	0.001	0.01 ±0 0.00

Post HD -tDCS

Parameters	Subject 1	Subject 2	Subject 3	Subject 4	Subject 5	Mean ± Std. Dev
a1	3.26	3.19	3.25	2.29	2.76	3.09 ± 0.21
a2	-3.79	-3.72	-3.74	-3.27	-2.98	-3.5 ± 0.36
a3	1.79	1.84	1.73	1.59	1.62	1.71 ± 0.10
a4	-0.26	-0.32	--0.24	-0.31	-0.40	-0.31 ± 0.06
b1	-0.013	0.008	-0.014	-0.134	0.0752	-0.02 ± 0.08
b2	0.029	-0.019	0.043	0.557	-0.006	0.12 ± 0.25
b3	-0.003	0.007	-0.029	-0.743	-0.225	-0.20 ± 0.32
b4	-0.028	0.009	-0.014	0.371	0.167	0.10 ± 0.17
b5	0..015	-0.006	0.014	-0.051	-0.006	0.01 ± 0.03

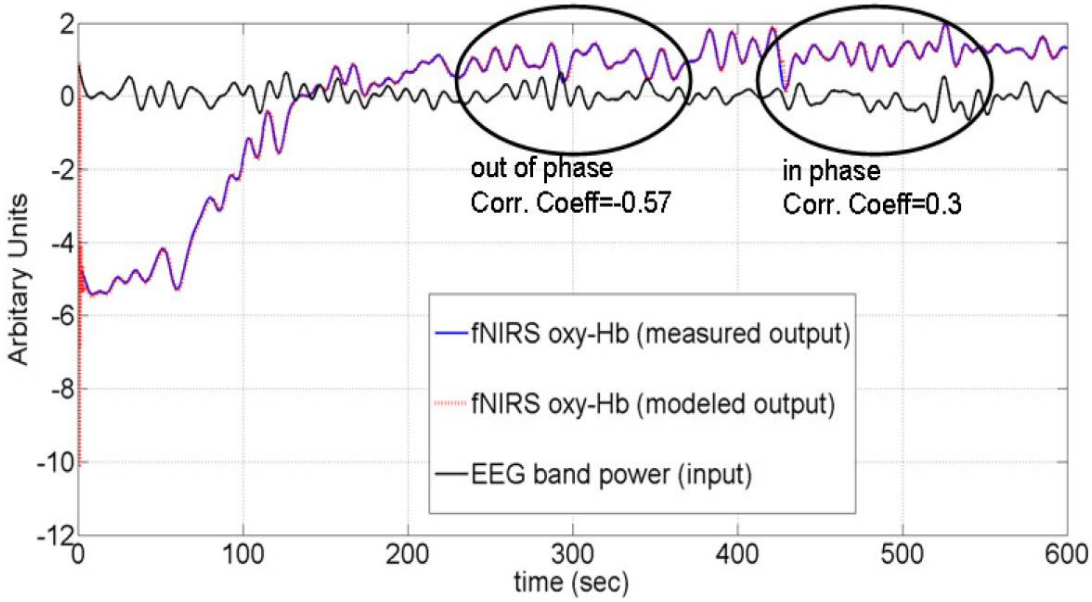

Fig 5.3 An example (subject 5) showing the EEG band (0.5-11.25 Hz) power as the input (in black), fNIRS oxy-Hb signal that was measured (in blue) as well as predicted by ARX online tracking method (in dotted red). Short-duration (~100sec) in phase and out of phase coupling between the fNIRS oxy-Hb signal and EEG band (0.5-11.25 Hz) power signals around 294sec and 428sec are shown that corresponded with the transients found in the ARX model parameters (see Figure 5.4).

5.3 Discussion

In this preliminary study on healthy, we presented Kalman Filter based online parameter estimation of an autoregressive (ARX) model with 4 poles, 6 zeros, and a constant dead time of 0.5sec to capture the transfer function from EEG band (0.5-11.25 Hz) power alterations to fNIRS oxy-Hb signal changes during HD-tDCS in the slow frequency regime (< 0.1 Hz). Here, online ARX parameter estimation with a Kalman filter provided a more convenient method to capture this time-varying transfer function when compared to sliding cross correlation calculations [18] where the choice of the window length and step size are subjective based upon visual observations of apparent relationships between the signals. Table 5.1 shows the transfer function at the start and at the end of HD-tDCS where the poles (a1, a2, a3, a4) are the roots of the denominator of the transfer function. Indeed, the poles associated with the output side have a direct influence on the dynamic properties of the system which were comparable across the healthy subjects' pre and post HD-tDCS. The zeros (b1, b2, b3, b4, b5) are the roots of the numerator of the transfer function which are associated with the input side, i.e., EEG band (0.5-11.25 Hz) power. The zeros varied during HD-tDCS, as shown in Table 5.1, which indicated HD-tDCS effects on the EEG band (0.5-11.25 Hz) power. Our online parameter estimation identified transient coupling relation between EEG power and oxy-Hb NIRS signals primarily with the alterations in the zeros(b1, b2, b3, b4, b5) of the transfer function when the cross-correlation (with around zero lag) between EEG band (0.5-11.25 Hz) power (as input) and fNIRS oxy-Hb signal (as output) in the slow frequency regime (< 0.1 Hz) fluctuated between negative correlation (top panel of Figure 5.4 (b)) and positive correlation (right panel of Figure 5.4 (b)) in a

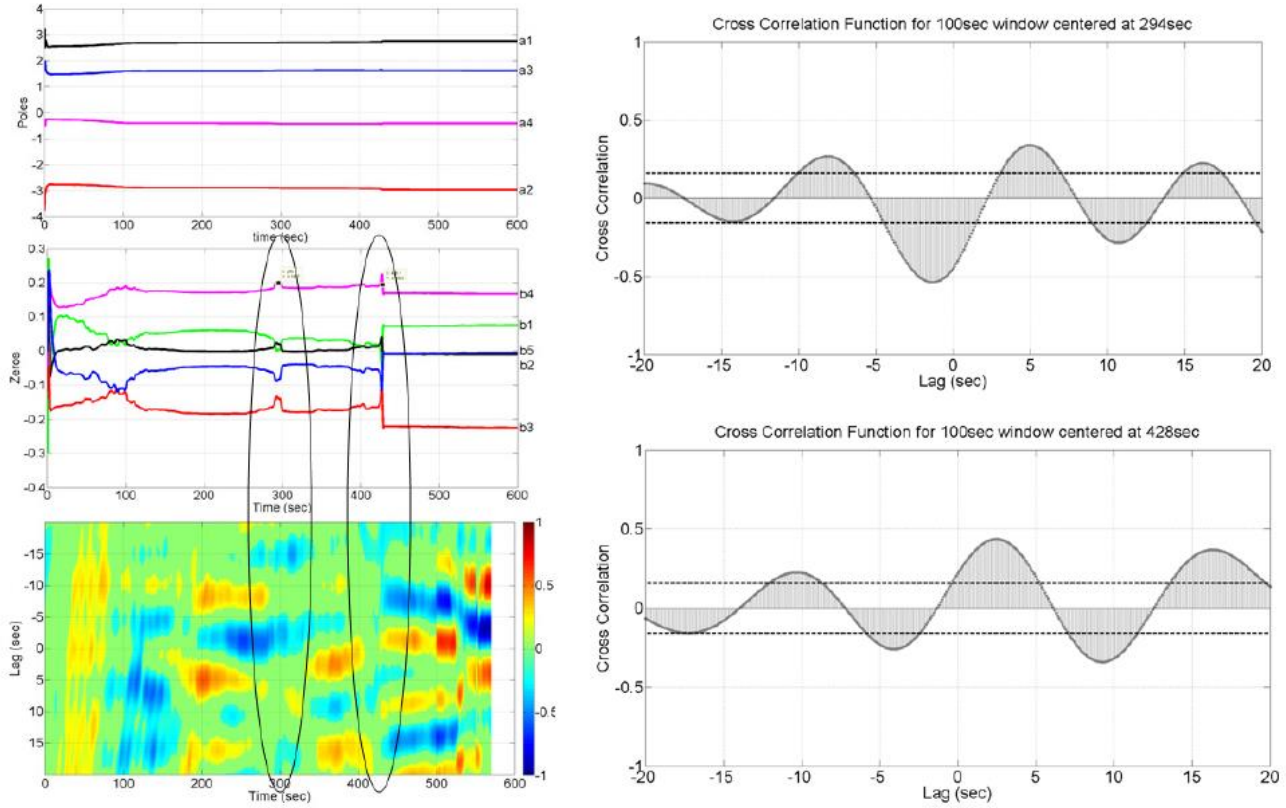

(a) (b)

Fig 5.4 a) An example (subject 5) of the correspondence between the ARX parameter tracking (time series of the poles and zeros shown in top two panels) and the sliding cross-correlation function (bottom panel) for fNIRS oxy-Hb signal as the output and EEG band (0.5-11.25 Hz) power as the input in the slow frequency regime (< 0.1 Hz). Transients (shown with ellipse) in the time-series of zeros (middle panel) can be found around 294sec and 428sec that corresponded with the sliding cross-correlation function (bottom panel).

b) Cross-correlation function shows short-duration (window length=100sec) negative coupling around 294sec (top panel) while positive coupling occurs around 428sec (bottom panel). Cross-correlation function measured the similarity between fNIRS oxy-Hb signal and 20sec shifted (lagged) copies of EEG band (0.5-11.25 Hz) power signal in the slow frequency regime (< 0.1 Hz) where the dashed horizontal lines show ±3 standard deviations for the estimation error assuming the signals to be uncorrelated.

healthy subject (Subject 5). Cross-correlation function (see Figure 1d) also demonstrated statistically significant (±3 standard deviations for the estimation error assuming the signals to be uncorrelated) cross-correlation at other lags which may be related to the transient bidirectional interactions [51] between the neuronal and hemodynamic components during HD-tDCS. Indeed, Dutta [26] postulated that since tDCS leads to increase in neuronal (synaptic) activity captured by EEG band power alterations [71] that require energy supply, glucose utilization, blood flow, and therefore changes fNIRS signal [72], however, such stimulation of glucose utilization in astrocytes can result in an increase in the extracellular lactate levels which when taken up by the neurons can

promote membrane depolarization, excitability alterations, and its after effects [73].Although low-dimensional physiological models of the neuro-glio-vascular unit may be necessary to elucidate such bidirectional interactions from multimodal neuroimaging data [74], nevertheless, system identification techniques presented in this paper may be more feasible for online tracking of this transient coupling between EEG band power and fNIRS oxy-Hb time-series that may provide a sensitive measure for titrating tDCSs' excitability alterations and after effects [75]. Moreover, subject-specific alterations of ARX poles and zeros with different dead time may be relevant for diagnosing neurovascular dysfunction since electrophysiological signatures of resting brain state [76] may be dysfunctional in cerebrovascular occlusive disease [77] which is also being investigated.

Chapter 6

Conclusions

Summary of the Present Work

In this thesis, we have employed Transcranial Direct Current Stimulation (tDCS) mainly for following two purposes:

1. For identification of the lesioned hemisphere in subacute stroke through the use of custom-built low cost NIRS- tDCS hardware. However, when using tDCS, there is a significant inter subject variability. Thus, it cannot be excluded that in certain stroke survivors, the lesioned hemisphere may not respond to anodal tDCS with an increase in neural activity. This may result in an absent change in the oxygen consumption as compared to the non-lesioned hemisphere. To avoid this potential problem, we employed EEG simultaneously with NIRS to record the changes in neural activity, as we hypothesized and later investigated that changes in EEG during tDCS are correlated with changes in NIRS, thus enabling us to measure the state of neurovascular coupling.

2. To understand the mechanism of neuro-modulation, which results into improvements in cognitive functioning. The role of hemodynamics during and after tDCS, which hasn't been studied well till date, has been researched along with the respective change in neural activity. This was done by developing a computational autoregressive (ARX) model for online parameter estimation with a Kalman Filter. This online parameter estimation can potentially track the transient coupling relation between EEG band power and oxy-Hb NIRS signals acquired simultaneously during anodal tDCS. As of now, the experiments were performed only on healthy subjects.

Future Work

If the NIRS-tDCS approach for identification of cerebrovascular status in stroke patients is verified by the future prospective multicenter trials, these findings may have important implications in both prognosis and rehabilitation of stroke survivors. The ARX parameter estimation with a Kalman Filter provided a very convenient and efficient way to capture the time-varying transfer function when compared to the conventional sliding window cross-correlation method. In future, this method can be investigated on stroke survivors and people with other neurovascular disorders.

The system identification techniques presented in this thesis may be more feasible for online tracking of the transient coupling between EEG band power and fNIRS oxy-Hb time series which might provide a sensitive measure for titrating tDCS's excitability alterations and after effects. The alterations due to subject variability in ARX poles and zeroes may prove to be relevant for diagnosing different neurological dysfunctionalities since the electrophysiological signatures of the resting brain state may be impaired in cerebrovascular occlusive diseases which can be further investigated. The physiological basis of the onset response of tDCS can be further investigated for monitoring the neuromodulatory effect in health and disease.

Related Publications

[1] M. Sood, U. Jindal, A. Das, A. Dutta, S. Roy Chowdhury, “Continuous wave functional near infra- red spectroscopy combined with transcranial direct current stimulation for assessment of cerebral vascular status in patients with ischemic stroke,” *fNIRS2014, At Montreal, Canada 2014*

[2] M. Sood, U. Jindal, S. Chowdhury, A. Das, D. Kondziella and A. Dutta, "Anterior temporal artery tap to identify systemic interference using short-separation NIRS measurements: A NIRS/EEG-tDCS study", *2015 37th Annual International Conference of the IEEE Engineering in Medicine and Biology Society (EMBC)*, 2015.

[3] M. Sood, U. Jindal, A. Das, S. Chowdhury, D. Kondziella and A. Dutta, "Modeling onset effects of transcranial direct current stimulation from NIRS-EEG joint-imaging : an ischemic stroke study", in *7th International IEEE EMBS Neural Engineering Conference*, Montpellier, France, 2016.

[4] U. Jindal, M. Sood, A. Dutta and S. Chowdhury, "Development of Point of Care Testing Device for Neurovascular Coupling From Simultaneous Recording of EEG and NIRS During Anodal Transcranial Direct Current Stimulation", *IEEE Journal of Translational Engineering in Health and Medicine*, vol. 3, pp. 1-12, 2015.

[5] U. Jindal, M. Sood, S. Chowdhury, A. Das, D. Kondziella and A. Dutta, "Corticospinal excitability changes to anodal tDCS elucidated with NIRS-EEG joint-imaging: An ischemic stroke study", *2015 37th Annual International Conference of the IEEE Engineering in Medicine and Biology Society (EMBC)*, 2015.

[6] U. Jindal, M. Sood, A. Das, S. Chowdhury and A. Dutta, "Near infra-red spectroscopy combined with transcranial direct current stimulation in FPGA-based hardware for point of care testing of cerebral vascular status - A stroke study", *2015 7th International IEEE/EMBS Conference on Neural Engineering (NER)*, 2015.

References:

[1] F. Fregni , M. A. Nitsche , C. K. Loo , A. R. Brunoni , P. Marangolo , J. Leite, S. Carvalho, N. Bolognini , W. Caumo , N. J. Paik, M. Simis, K. Ueda, H. Ekhtiari, P. Luu, D. M. Tucker, W. J. Tyler, J. Brunelin, A. Datta, C. H. Juan, G. Venkatasubramanian, P. S. Boggio, and M. Bikson. (2014) "Regulatory considerations for the clinical and research use of transcranial direct current stimulation (tDCS): Review and recommendations from an expert panel". *Informa Healthcare USA, Inc. DOI: 10.3109/10601333.2015.980944*

[2] V. Walsh and A. Cowey, "Transcranial magnetic stimulation and cognitive neuroscience," *Nat. Rev. Neurosci.*, vol. 1, no.1, pp. 73–79, Oct. 2000.

[3] Priori A, Hallett M, Rothwell JC. (2009) "Repetitive transcranial magnetic stimulation or transcranial direct current stimulation Brain Stimuli" *(4):241–245. [PubMed]*

[4] Nitsche MA, Cohen LG, Wassermann EM, Priori A, Lang N, Antal A, et al.(2008) "Transcranial direct current stimulation*" State of the art BRAIN STIMULATION.1(3):206–223. [PubMed]*

[5] Andre Russowsky Brunoni, Michael A. Nitsche, Nadia Bolognini, Marom Bikson, Tim Wagner, Lotfi Merabet, Dylan J. Edwards, Antoni Valero-Cabre, Alexander Rotenberg, Alvaro Pascual-Leone, Roberta Ferrucci, Alberto Priori, Paulo Boggio, and Felipe Fregni (2011). "Clinical Research with Transcranial Direct Current Stimulation (tDCS): Challenges and Future Directions."*doi: 10.1016/j.brs.2011.03.002 PMCID: PMC3270156 , NIHMSID: NIHMS283820*

[6] M. A. Nitsche and W. Paulus, "Excitability changes induced in the human motor cortex by weak transcranial direct current stimulation," *J. Physiol., vol. 527, no. 3, pp. 633–639, Sep*. 2000.

[7] Nicolas Lang, Hartwig R. Siebner, Nick S. Ward, Lucy Lee, Michael A. Nitsche, Walter Paulus, John C. Rothwell, Roger N. Lemon and Richard S. Frackowiak "How does transcranial DC stimulation of the primary motor cortex alter regional neuronal activity in the human brain", *European Journal of Neuroscience* Volume 22, Issue 2, pages 495–504, July 2005

[8] H. Girouard and C. Iadecola, "Neurovascular coupling in the normal brain and in hypertension, stroke, and Alzheimer disease," *J. Appl. Physiol. Bethesda Md 1985*, vol. 100, no. 1, pp. 328–335, Jan. 2006.

[9] Borckardt, Jeffrey J.; Bikson, Marom; Frohman, Heather; Reeves, Scott T.; Datta, Abhishek; Bansal, Varun; Madan, Alok; Barth, Kelly; George, Mark S. (2012). "A Pilot Study of the

Tolerability and Effects of High-Definition Transcranial Direct Current Stimulation (HD-tDCS) on Pain Perception". *The Journal of Pain 13 (2): 11220.doi:10.1016/j.jpain.2011.07.001. PMID 22104190*

[10] Fregni F, Liebetanz D, Monte-Silva KK, Oliveira MB, Santos AA, Nitsche MA, et al. (2007), "Effects of transcranial direct current stimulation coupled with repetitive electrical stimulation on cortical spreading depression." *Exp Neurol. Mar;204(1):462–466. [PubMed*]

[11] Michael A. Nitsche. Charlotte J. Stagg . Physiological Basis of Transcranial Direct Current Stimulation, *Neuroscientist, 17* (2011*), pp. 37–53*

[12] Hoy, K. E., Arnold, S. L., Emonson, M. R., Daskalakis, Z. J., and Fitzgerald, P. B. (2014). "An investigation into the effects of tDCS dose on cognitive performance over time in patients with schizophrenia. Schizophr." *Res. 155, 96–100. doi: 10.1016/j.schres.2014.03.006*

[13] Sanne Koops,Hilde van den Brink, " Transcranial direct current stimulation as a treatment for auditory hallucinations ". *Psychiatry Department, Brain Center Rudolf Magnus, University Medical Center Utrecht, Utrecht, Netherlands http://dx.doi.org/10.3389/fpsyg.2015.00244*

[14] Datta, Abhishek; Bansal, Varun; Diaz, Julian; Patel, Jinal; Reato, Davide; Bikson, Marom (2009). "Gyri-precise head model of transcranial direct current stimulation: Improved spatial focality using a ring electrode versus conventional rectangular pad". *Brain Stimulation 2 (4): 201–7, 207.e1. doi:10.1016/j.brs.2009.03.005. PMC 2790295.PMID 20648973*

[15] Kuo, Hsiao-I.; Bikson, Marom; Datta, Abhishek; Minhas, Preet; Paulus, Walter; Kuo, Min-Fang; Nitsche, Michael A. (2013). "Comparing Cortical Plasticity Induced by Conventional and High-Definition 4 × 1 Ring tDCS: A Neurophysiological Study". Brain Stimulation 6 (4): *644–8. doi:10.1016/j.brs.2012.09.010. PMID 23149292*

[16] Helfrich RF, Schneider TR, Rach S, Trautmann-Lengsfeld SA, Engel AK, Herrmann CS (2014) " Entrainment of brain oscillations by transcranial alternating current stimulation" *Current biology CB 24(3):333–339. doi:10.1016/j.cub.2013.12.041*

[17] Terney D, Chaieb L, Moliadze V, Antal A, Paulus W (2008) "Increasing human brain excitability by transcranial high-frequency random noise stimulation." *The Journal of neuroscience : the official journal of the Society for Neuroscience 28(52):14147–14155. doi:10.1523/JNEUROSCI.4248-08.2008*

[18] Zaghi S, Acar M, Hultgren B, Boggio PS, Fregni F.(2009) " Noninvasive Brain Stimulation with Low-Intensity Electrical Currents: Putative Mechanisms of Action for Direct and Alternating Current Stimulation.Neuroscientist" *[PubMed]*

[19] Liebetanz D, Koch R, Mayenfels S, Konig F, Paulus W, Nitsche MA. (2009) "Safety limits of cathodal transcranial direct current stimulation in rats." Clin Neurophysiol.*1161–1167. [PubMed]*

[20] Brunoni, A. R., Nitsche, M. A., Bolognini, N., Bikson, M., Wagner, T., Merabet, L. Fregni, F. (2012). Clinical Research with Transcranial Direct Current Stimulation (tDCS): Challenges and Future Directions. *Brain Stimulation, 5*(3), 175–195.http://doi.org/10.1016/j.brs.2011.03.002

[21] A. Dutta, "Bidirectional interactions between neuronal and hemodynamic responses to transcranial direct current stimulation (tDCS): challenges for brain-state dependent tDCS," *Front. Syst. Neurosci., p. 107,* 2015

[22] D. P. Subha, P. K. Joseph, R. Acharya U, and C. M. Lim, "EEG signal analysis: a survey*," J.Med. Syst., vol. 34, no. 2, pp. 195–212,* Apr. 2010.

[23] S. Coyle, T. Ward, C. Markham, and G. McDarby, "On the suitability of near-infrared (NIR) systems for next-generation brain-computer interfaces," *Physiol. Meas., vol. 25, no. 4, pp. 815–822,* Aug. 2004.

[24] Flavia Mengarelli, Silvia Spoglianti, Alessio Avenanti and Giuseppe di Pellegrino "Cathodal tDCS Over the Left Prefrontal Cortex Diminishes Choice-Induced Preference Change".

[25] M. Bikson and A. Datta, "Guidelines for precise and accurate computational models of tDCS," *Brain Stimulat., vol. 5, no. 3, pp. 430–431,* Jul. 2012.

[26] A. Dutta, A. Jacob, S. R. Chowdhury, A. Das, and M.A. Nitsche, "EEG-NIRS Based Assessment of Neurovascular Coupling During Anodal Transcranial Direct Current Stimulation - a Stroke Case Series," *J. Med. Syst., vol. 39, no. 4, p. 205,* Apr. 2015

[27] S. Lloyd-Fox, A. Blasi, and C. E. Elwell, "Illuminating the developing brain: the past, present and future of functional near infrared spectroscopy," *Neurosci. Biobehav. Rev.,* vol. 34, no. 3, pp. 269–284, Mar. 2010.

[28] M. Douds, E. Straub, A. Kent, C. Bistrick, and J. Sistino, "A systematic review of cerebral oxygenation-monitoring devices in cardiac surgery," *Perfusion,* Jul. 2014.

[29] A. Villringer and B. Chance, "Non-invasive optical spectroscopy and imaging of human brain function," *Trends Neurosci.*, vol. 20, no. 10, pp. 435–442, Oct. 1997.

[30] D. T. Delpy, M. Cope, P. van der Zee, S. Arridge, S. Wray, and J. Wyatt, "Estimation of optical pathlength through tissue from direct time of flight measurement," *Phys. Med. Biol.*, vol. 33, no. 12, pp. 1433–1442, Dec. 1988.

[31] L. B. Goldstein, "Should antihypertensive therapies be given to patients with acute ischemic stroke?" *Drug Saf* 22(1), 13–18 (2000).

[32] J.A. Filosa, "Vascular tone and neurovascular coupling: considerations toward an improved in vitro model", *Front. Neuroenergetics.* 2(16), 1–8 (2010).

[33] W.H. Lin, Q. Hao, B. Rosengarten, W.H. Leung, K.S. Wong, "Impaired neurovascular coupling in ischaemic stroke patients with large or small vessel disease", *Eur. J. Neurol.* 18(5), 731–736 (2011).

[34] M. Hiraoka, M. Firbank, M. Essenpreis, M. Cope, S. R. Arridge, P. van der Zee, and D. T. Delpy, "A Monte Carlo investigation of optical pathlength in inhomogeneous tissue and its application to near-infrared spectroscopy," *Phys. Med. Biol.*, vol. 38, no. 12, pp. 1859–1876, Dec. 1993.

[35] Cope,M.: The application of near-infrared spectroscopy to non-invasive monitoring of cerebral oxygenation in the newborn infant. *PhD thesis, University of London* (1991)

[36] U. Jindal, M. Sood, A. Dutta, and S. R. Chowdhury, "Development of Point of Care Testing Device for Neurovascular Coupling From Simultaneous Recording of EEG and NIRS During Anodal Transcranial Direct Current Stimulation," *IEEE J. Transl. Eng. Health Med.*, vol. 3, pp. 1–12, 2015

[37] L. Gagnon, R. J. Cooper, M. A. Yucel, K. L. Perdue, D. N. Greve, and D. A. Boas, "Short separation channel location impacts the performance of short channel regression in NIRS," *NeuroImage*, vol. 59, no. 3, pp. 2518–2528, Feb. 2012.

[38] P. Schestatsky, L. Morales-Quezada, and F. Fregni, "Simultaneous EEG Monitoring During Transcranial Direct Current Stimulation," *J. Vis. Exp. JoVE*, no. 76, Jun. 2013.

[39] A. Dutta, A. Jacob, S. R. Chowdhury, A. Das, and M. A. Nitsche, "EEG-NIRS Based Assessment of Neurovascular Coupling During Anodal Transcranial Direct Current Stimulation - a Stroke Case Series," *J. Med. Syst.*, vol. 39, no. 4, p. 205, Apr. 2015.

[40] A. Delorme and S. Makeig, "EEGLAB: an open source toolbox for analysis of single-trial EEG dynamics including independent component analysis," *J. Neurosci. Methods*, vol. 134, no. 1, pp. 9–21, Mar. 2004.

[41] A. Dutta, "EEG-NIRS based low-cost screening and monitoring of cerebral microvessels functionality," *International Stroke Conference*, San Diego, California, February 6-8, 2014.

[42] K. Jann, T. Koenig, T. Dierks, C. Boesch, and A. Federspiel, "Association of individual resting state EEG alpha frequency and cerebral blood flow," *NeuroImage*, vol. 51, no. 1, pp. 365–372, May 2010.

[43] H. Markus and M. Cullinane, "Severely impaired cerebrovascular reactivity predicts stroke and TIA risk in patients with carotid artery stenosis and occlusion," *Brain*, vol. 124, no. 3, pp. 457–467, Mar. 2001.

[44] E. Vicenzini, M. C. Ricciardi, M. Altieri, F. Puccinelli, N. Bonaffini, V. Di Piero, and G. L. Lenzi, "Cerebrovascular reactivity in degenerative and vascular dementia: a transcranial Doppler study," *Eur. Neurol.*, vol. 58, no. 2, pp. 84–89, 2007.

[45] A. Gupta, J. L. Chazen, M. Hartman, D. Delgado, N. Anumula, H. Shao, M. Mazumdar, A. Z. Segal, H. Kamel, D. Leifer, and P. C. Sanelli, "Cerebrovascular reserve and stroke risk in patients with carotid stenosis or occlusion: a systematic review and meta-analysis," *Stroke J. Cereb. Circ.*, vol. 43, no. 11, pp. 2884–2891, Nov. 2012.

[46] X. Zheng, D. C. Alsop, and G. Schlaug, "Effects of transcranial direct current stimulation (tDCS) on human regional cerebral blood flow," *NeuroImage*, vol. 58, no. 1, pp. 26–33, Sep. 2011.

[47] A. Dutta, A. Jacob, S. R. Chowdhury, A. Das, and M. A. Nitsche, "EEG-NIRS Based Assessment of Neurovascular Coupling During Anodal Transcranial Direct Current Stimulation - a Stroke Case Series," *J. Med. Syst.*, vol. 39, no. 4, p. 205, Apr. 2015.

[48] H. Girouard and C. Iadecola, "Neurovascular coupling in the normal brain and in hypertension, stroke, and Alzheimer disease," *J. Appl. Physiol. Bethesda Md 1985*, vol. 100, no. 1, pp. 328–335, Jan. 2006.

[49] A. Devor, S. Sakadžić, V. J. Srinivasan, M. A. Yaseen, K. Nizar, P. A. Saisan, P. Tian, A. M. Dale, S. A. Vinogradov, M.A. Franceschini, and D. A. Boas, "Frontiers in optical imaging of cerebral blood flow and metabolism," *J. Cereb. Blood Flow Metab. Off. J. Int. Soc. Cereb. Blood Flow Metab.*, vol. 32, no. 7, pp. 1259–1276, Jul. 2012.

[50] M. Muthalib, P. Besson, J. Rothwell, T. Ward, and S. Perrey, “Effects of Anodal High-Definition Transcranial Direct Current Stimulation on Bilateral Sensorimotor Cortex Activation During Sequential Finger Movements: An fNIRS Study,” *Adv. Exp. Med. Biol.*, vol. 876, pp. 351–359, 2016.

[51] A. Dutta, “Bidirectional interactions between neuronal and hemodynamic responses to transcranial direct current stimulation (tDCS): challenges for brain-state dependent tDCS,” *Front. Syst. Neurosci.*, p. 107, 2015.

[52] A. Dutta, A. Jacob, S. R. Chowdhury, A. Das, and M. A. Nitsche, “EEG-NIRS Based Assessment of Neurovascular Coupling During Anodal Transcranial Direct Current Stimulation - a Stroke Case Series,” *J. Med. Syst.*, vol. 39, no. 4, p. 205, Apr. 2015.

[53] G. Pfurtscheller, I. Daly, G. Bauernfeind, and G. R. Muller-Putz, “Coupling between intrinsic prefrontal HbO2 and central EEG beta power oscillations in the resting brain,” *PloS One*, vol. 7, no. 8, p. e43640, 2012.

[54] V. V. Nikulin, T. Fedele, J. Mehnert, A. Lipp, C. Noack, J. Steinbrink, and G. Curio, “Monochromatic Ultra-Slow (~0.1Hz) Oscillations in the human electroencephalogram and their relation to hemodynamics,” *NeuroImage*, Apr. 2014.

[55] P. L. Nunez and R. Srinivasan, *Electric Fields of the Brain: The Neurophysics of EEG*. Oxford University Press, 2006.

[56] “EEG: MedlinePlus Medical Encyclopedia.” [Online]. Available: https://www.nlm.nih.gov/medlineplus/ency/article/003931.htm. [Accessed: 21-Sep-2015].

[57] S. L. Dawson, R. B. Panerai, and J. F. Potter, “Serial changes in static and dynamic cerebral autoregulation after acute ischaemic stroke,” *Cerebrovasc Dis* 16(1), 69–75 (2003).

[58] “The Neurophysiological Biomarker Toolbox (NBT) [NBTwiki.net].” [Online]. Available: https://www.nbtwiki.net/. [Accessed: 21-Sep-2015].

[59] P. L. Nunez and R. Srinivasan, *Electric Fields of the Brain: The Neurophysics of EEG*. Oxford University Press, 2006.

[60]“EEG: MedlinePlus Medical Encyclopedia.” [Online]. Available: https://www.nlm.nih.gov/medlineplus/ency/article/003931.htm. [Accessed: 21-Sep-2015].

[61] M. Tudor, L. Tudor, and K. I. Tudor, "[Hans Berger (1873-1941)--the history of electroencephalography]," *Acta Medica Croat. Č asopis Hravatske Akad. Med. Znan.*, vol. 59, no. 4, pp. 307–313, 2005.

[62] G. Pfurtscheller, I. Daly, G. Bauernfeind, and G. R. Muller-Putz, "Coupling between intrinsic prefrontal HbO2 and central EEG beta power oscillations in the resting brain," *PloS One*, vol. 7, no. 8, p. e43640, 2012.

[63] B. S. Chander and V. S. Chakravarthy, "A Computational Model of Neuro-Glio Vascular Loop Interactions," *PLoS One*, vol. 7, no. 11, p. e48802, Nov. 2012.

[64] V. V. Nikulin, T. Fedele, J. Mehnert, A. Lipp, C. Noack, J. Steinbrink, and G. Curio"Monochromatic Ultra-Slow (~0.1Hz) Oscillations in the human electroencephalogram and their relation to hemodynamics," *NeuroImage*, Apr. 2014.

[65] C. Julien, "The enigma of Mayer waves: Facts and models," *Cardiovasc. Res.*, vol. 70, no. 1, pp. 12–21, Apr. 2006.

[66] A. Dutta, A. Jacob, S. R. Chowdhury, A. Das, and M. A. Nitsche, "EEG-NIRS Based Assessment of Neurovascular Coupling During Anodal Transcranial Direct Current Stimulation - a Stroke Case Series," *J. Med. Syst.*, vol. 39, no. 4, p. 205, Apr. 2015.

[67] X.-S. Hu, K.-S. Hong, S. S. Ge, and M.-Y. Jeong, "Kalman estimator- and general linear model-based on-line brain activation mapping by near-infrared spectroscopy," *Biomed. Eng. Online*, vol. 9, p. 82, 2010.

[68] Q. Zhang, M. Hayashibe, P. Fraisse, and D. Guiraud, "FES-Induced Torque Prediction With Evoked EMG Sensing for Muscle Fatigue Tracking," *IEEEASME Trans. Mechatron.*, vol. 16, no. 5, pp. 816–826, Oct. 2011.

[69] Q. Zhang, M. Hayashibe, P. Fraisse, and D. Guiraud, "FES-Induced Torque Prediction With Evoked EMG Sensing for Muscle Fatigue Tracking," *IEEEASME Trans. Mechatron.*, vol. 16, no. 5, pp. 816–826, Oct. 2011.

[70] A. Delorme and S. Makeig, "EEGLAB: an open source toolbox for analysis of single-trial EEG dynamics including independent component analysis," *J. Neurosci. Methods*, vol. 134, no. 1, pp. 9–21, Mar. 2004.

[71] A. Dutta and M. . Nitsche, "Neural mass model analysis of online modulation of electroencephalogram with transcranial direct current stimulation," in *2013 6th International IEEE/EMBS Conference on Neural Engineering (NER)*, 2013, pp. 206–210.

[72] A. Dutta, S. R. Chowdhury, A. Dutta, P. N. Sylaja, D. Guiraud, and M. . Nitsche, "A phenomological model for capturing cerebrovascular reactivity to anodal transcranial direct current stimulation," in *2013 6th International IEEE/EMBS Conference on Neural Engineering (NER)*, 2013, pp. 827–830.

[73] B. S. Chander and V. S. Chakravarthy, "A Computational Model of Neuro-Glio-Vascular Loop Interactions," *PLoS One*, vol. 7, no. 11, p. e48802, Nov. 2012.

[74] K. Chhabria and V. S. Chakravarthy, "Low-Dimensional Models of 'Neuro-Glio-Vascular Unit' for Describing Neural Dynamics under Normal and Energy-Starved Conditions," *Stroke*, p. 24, 2016.

[75] U. Jindal, M. Sood, S. R. Chowdhury, A. Das, D. Kondziella, and A. Dutta, "Corticospinal excitability changes to anodal tDCS elucidated with NIRS-EEG joint-imaging: An ischemic stroke study," *Conf. Proc. Annu. Int. Conf. IEEE Eng. Med. Biol. Soc. IEEE Eng. Med. Biol. Soc. Annu. Conf.*, vol. 2015, pp. 3399–3402, Aug. 2015.

[76] D. Mantini, M. G. Perrucci, C. Del Gratta, G. L. Romani, and M. Corbetta, "Electrophysiological signatures of resting state networks in the human brain," *Proc. Natl. Acad. Sci. U. S. A.*, vol. 104, no. 32, pp. 13170–13175, Aug. 2007.

[77] D. Phillip, H. K. Iversen, H. W. Schytz, J. Selb, D. A. Boas, and M. Ashina, "Altered Low Frequency Oscillations of Cortical Vessels in Patients with Cerebrovascular Occlusive Disease – A NIRS Study," *Front. Neurol.*, vol. 4, Dec. 2013.